Normal and shear stresses between a rigid sphere and an elastic half-space
by James Martin Alzheimer

A thesis submitted in partial fulfillment of the requirements for the degree of MASTER OF SCIENCE
in Mechanical Engineering
Montana State University

Abstract:
The frictional contact problem between a rigid sphere and an elastic half-space has been modeled using a form of the collocation technique in which the surface stresses have been approximated by a series of disk loadings. A computer program has been written using these methods to find the surface shear stresses, the surface normal stresses and the surface displacements for a given set of physical properties and a given coefficient of friction. The effects of various coefficients of friction on the stresses and displacements have been predicted. For the first time it was possible to approximate the surface shear stresses.

NORMAL AND SHEAR STRESSES BETWEEN A RIGID SPHERE AND AN ELASTIC HALF-SPACE

by

JAMES MARTIN ALZHEIMER

A thesis submitted in partial fulfillment
of the requirements for the degree

of

MASTER OF SCIENCE

in

Mechanical Engineering

Approved:

Harry W. Tourna
Chairman, Examining Committee

Dennis O. Blackketter
Head, Major Department

Henry L Parsons
Graduate Dean

MONTANA STATE UNIVERSITY
Bozeman, Montana

February, 1976

STATEMENT OF PERMISSION TO COPY

In presenting this thesis in partial fulfillment of of the requirements for an advanced degree at Montana State University, I agree that the Library shall make it freely available for inspection. I further agree that permission for extensive copying of this thesis for scholarly purposes may be granted by my major professor, or, in his absence, by the Director of Libraries. It is understood that any copying or publication on this thesis for financial gain shall not be allowed without my permission.

James Martin Oltheuin
Name

February 9, 1976
Date

ACKNOWLEDGEMENT

The author is indebted to Dr. H.W. Townes for his valuable assistance in this work.

The support of the Department of Mechanical Engineering is appreciated.

The author also expresses gratitude to his fiancee and to his parents for their patience, understanding and support.

TABLE OF CONTENTS

TABLE OF CONTENTS
(continued)

LIST OF TABLES

LIST OF FIGURES

LIST OF FIGURES
(continued)

Chapter 1

INTRODUCTION

Many machine elements make contact over extremely small areas, for example cams, gears and bearings. One member of this group for which stresses rise steeply in the vicinity of the contact region is ball bearings. Since bearing failure is related to both the normal and shear stresses, the contact stresses are a major factor for the determination of the life of ball bearing elements.

The work presented here not only treats the non-conformal contact stress problem, as has been the case in most past investigations, but also includes the effects of surface friction. Curved surfaces are non-conformal if all dimensions of the contact region are small compared to the smallest radius of curvature of either of the surfaces. Most bodies can be treated as non-conformal as long as there are no sharp changes on the surface. The assumption of non-conformal surfaces allows the contacting elements to be treated as flat plates as far as the stress-strain relationships are concerned.

The problem of contact stresses in the case of three dimensional elastic surfaces has been studied by several investigators. Hertz (6) solved the three dimensional

problem of contacting, non-conformal, frictionless elastic surfaces for the class of surfaces that can be modeled as quadratic near the contact point. A considerable number of investigators have expanded Hertz's work in an effort to solve problems that can not be modeled as quadratic surfaces. Mow, Chow and Ling (13) assumed the surfaces to be fourth order parabaloids and had some limited success. Cattaneo (4) solved the axi-symmetric contact problem for the special case in which the 'profile function' (profile function is defined in the next chapter) is given by

$$F = A1*R**2 + A2*R**4 \quad (1.1)$$ †

Blackketter (2) developed a method for determining the contact stresses between finite two-dimensional elastic bodies in which the surfaces considered are nearly rectangular with small deviations from the rectangular shape. Conry and Seireg (5) proposed a solution, using linear programming, in which a number of candidate points were picked on the contact surface, and the pressure distribution is approximated by discrete forces at these points. Kalker and Randen (7) proposed a general variational principle for both linear and nonlinear elastic contact.

Singh (15) devised a method to solve the contact

† All equations are written using FORTRAN language

problem in which the surfaces are frictionless and non-conformal but otherwise arbitrary. In his work the contact region was divided into cells and the normal stress distribution was approximated by a constant pressure inside each cell. With this technique Singh was able to solve a large number of contact problems, although he found the problems to be 'ill posed' in the sense that numerical difficulties were present.

In the work described in this thesis a formulation of the problem of a rigid sphere in contact with an elastic half-space is made. The surfaces are non-conformal and can be modeled as quadratic as in Hertz's work, but the surfaces are not frictionless. Whereas previous work has dealt mainly with frictionless surfaces and therefore only considered normal surface stresses, the present work deals with the prediction of the normal stress, shear stress and the slip-stick region. Typical values of sliding coefficients of friction for metals in contact range from 0.04 to over 1.0. The value of the coefficient of friction can have a significant effect on the contact stresses.

The problem considered here is that of a rigid sphere in contact with an elastic half-space. The sphere is not allowed to rotate and the only relative motion between the

two bodies is a rigid body translation of the sphere toward the half-space. A rigid sphere is used in order to simplify the problem. In addition a rigid sphere causes the maximum shear stress between the two surfaces. The problem posed is seen as the first step in the prediction of the surface stresses between the rolling ball and the race in a ball bearing.

The method used for the solution of the problem is a form of the collocation technique in which the stress distributions will be approximated by a series of circular disk loads. In this method the displacements of the half-space are initially assumed known. Using these 'known' displacements the stresses are found. A method is then devised to approximate the surface displacements by a stepping process.

Chapter 2

FORMULATION OF THE CONTACT PROBLEM BETWEEN A RIGID SPHERE AND AN ELASTIC HALF-SPACE

2.1 The Physical System To Be Modeled

As was stated in the introduction, the system considered is that of a rigid sphere and an elastic half-space. Cylindrical coordinates are used to describe the system, as shown in Figure 1, with the origin at the initial contact point. The R and θ axes lie in the surface plane of the half-space and the Z axis is positive into the half-space. The radius of the sphere is R1. The distance from the half-space to the sphere as measured in the Z direction is a function of the radial distance R from the origin and is known as the profile function F which is given by

$$F(R) = R1 - SQRT(R1**2 - R**2) \qquad (2.1)$$

If an external force acting along the Z axis is applied to the center of the sphere, this force tends to push the sphere into the half-space and deform the surface of the half-space. The two bodies are no longer in contact at a point but are in contact over a circular region. Since the problem is axially symmetric, displacements of the half-space are in the R and Z directions only. As the half-space deforms stresses develop in the half-

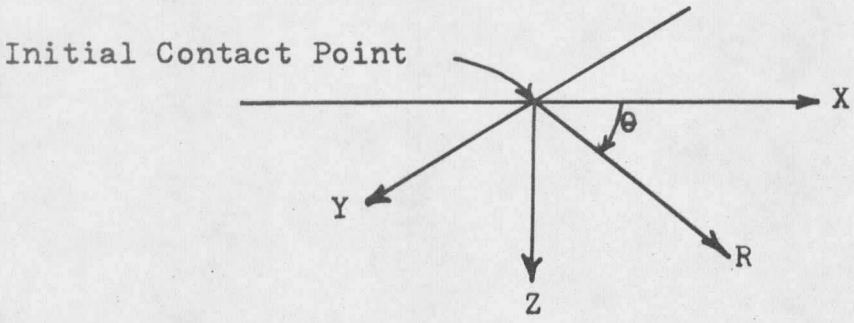

Figure 1
Cylindrical Coordinate System In Half-space

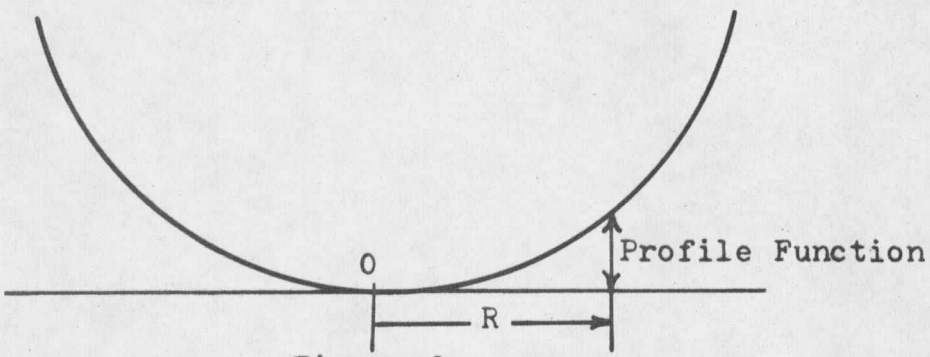

Figure 2
Profile Function Between A Sphere And Half-space

space and between the two bodies, which include both normal and shear stresses.

The force resulting from the integral of surface stresses over the contact region is equal in magnitude to the externally applied force.

Surface shear stresses develop between the rigid sphere and the elastic half-space since the half-space tends to be pushed away from the origin in the radial direction. Friction between the sphere and half-space tends to keep that part of the half-space in contact with the rigid sphere from moving. If both bodies were of the same material and therefore had the same elastic properties, no surface shear stresses would be developed since each would have the same radial displacements. The radial displacements would be the same for each body if the problem is considered as non-conformal. With the assumption of non-conformality the displacements are those of a half-space in both the sphere and half-space. If both bodies were elastic but with different properties, surface shear stresses would develop, but the shear stresses would not be as large as in the case of a rigid sphere and an elastic half-space. As the approach distance is increased, points on the surface of the half-space not in the contact region

are displaced in the radial and normal directions. When these points eventually are included in the contact region their previous displacements have an effect upon the stresses. The stresses, displacements and prior history of motion can not be treated independently. They are interrelated and it is this interrelationship which leads to difficulties in developing a numerical procedure to solve the problem. If either the stresses or the displacements are known, solution of the problem is straight forward.

2.2 Method Used To Find The Surface Stresses If The Surface Displacements Are Known

One aspect of the problem is the determination of the displacements and stresses for a given set of elastic properties and a given coefficient of friction between the two bodies. The procedure used is as follows.

Initially it is assumed that the displacements of the half-space surface in the R and Z directions are known. With these 'known' displacements an approximation of the normal and shear stress distributions is made. The method used for this approximation is a form of the collocation technique, for which the contact region is divided into N annular regions and in each region there is a collocation point as shown in Figure 3. The normal and radial

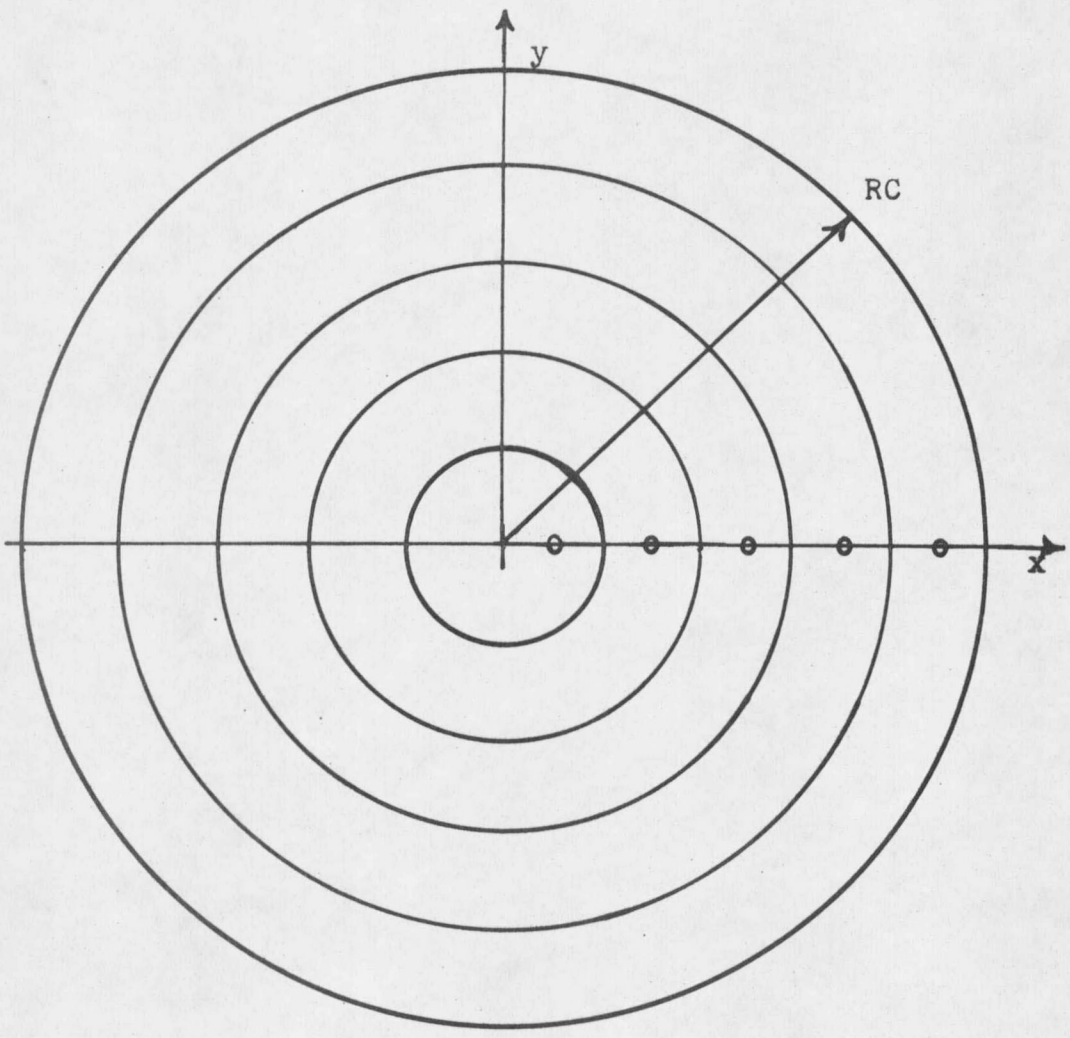

Collocation Point o

Figure 3

View Of Surface Of Half-space Showing
Collocation Points And Disk Circles
N = 5

displacements at these N collocation points are treated as known and the stresses in the N annular regions are treated as unknowns. The radius to the outside edge of an annular region is RD(J) and a collocation point is a distance R(I) from the origin. The RD(J)'s are picked such that the width of the rings is constant. The collocation points are at the center of each ring.

Attempts to use different configurations did not result in any improvement in predicted stresses and usually resulted in higher computing time or inability to solve the equations. With the collocation method an equation is written expressing the displacement at each collocation point in terms of the stress distribution in each of the annular regions. Each equation has N unknown normal stresses and N unknown shear stresses. There are two equations for each of the collocation points, one for the radial displacement and one for the normal displacement. This results in 2 N equations in 2 N unknowns.

The normal and shear stress distributions are approximated by a series of circular disk loadings. The normal stress distribution is approximated by a series of N uniform disk stresses of radii RD(J) and stress level P(J). The shear stress distribution is approximated by N shear stress

disks of radii RD(J). These shear stress disks have zero shear stress at the center and the stress increases linearly to a shear stress of Q(J) at the outside edge as shown in Figure 4. Each stress disk has a radius corresponding to one of the annular collocation regions.

These particular stress distributions are chosen because the contact problem is axially symmetric and these stress distributions can be combined to approximate the expected stress distribution which is shown in Figure 5. The normal stress distribution is expected to have its maximum value at the center and zero at the outside edge. The expected shear stress distribution has a zero value at the center and outside edge and a maximum value in the interior.

Both the normal and shear stresses make a contribution to both the normal and radial displacements. The displacements at a point due to one of the disk loads is a function of the type of loading, either shear or normal, the direction of the displacement, the radius to the collocation point, the radius of the disk load, and the magnitude of the disk load. Since the problem is linear, the displacement at a point due to a load is directly proportional to the magnitude of the load. Therefore if the displacement at a

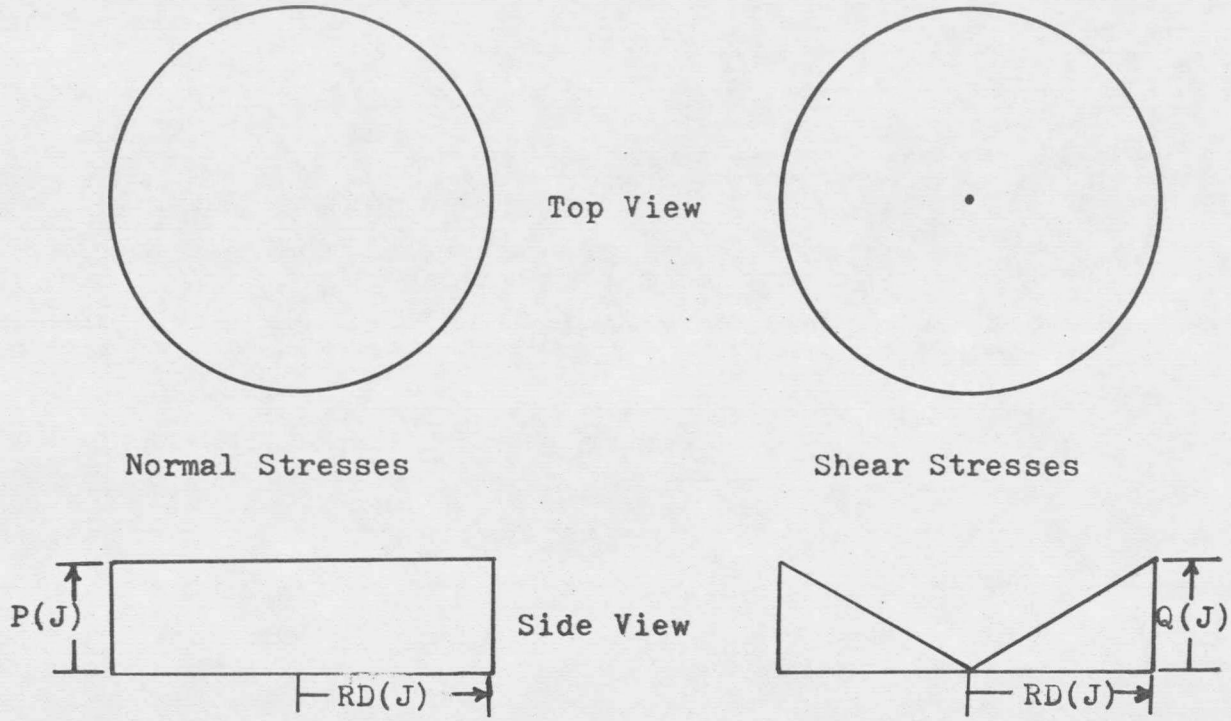

Figure 4
Shapes Of Disk Loadings

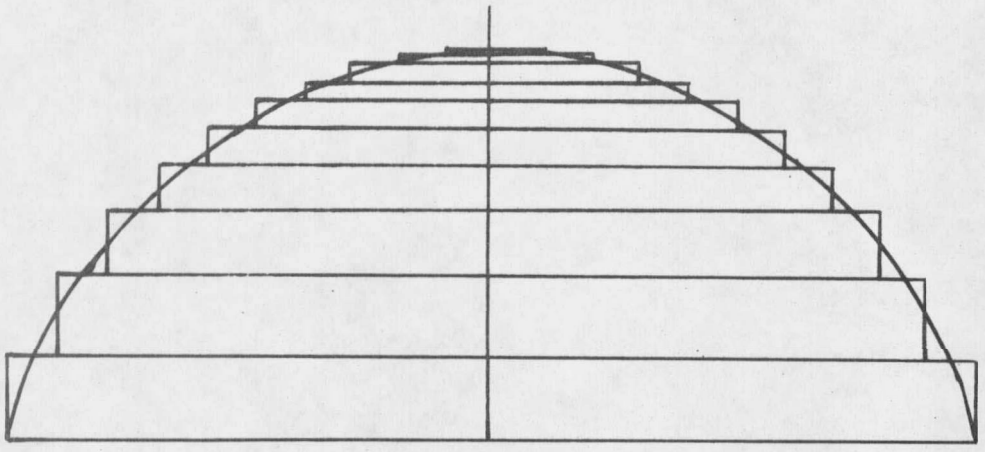

Approximation To Expected Normal Stress Distribution

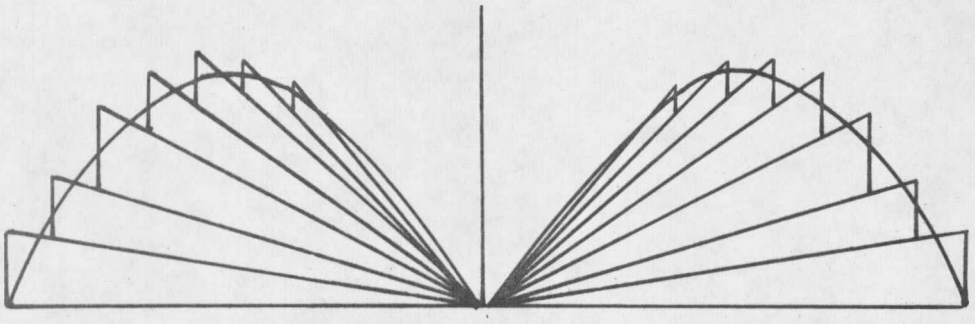

Approximation To Expected Shear Stress Distribution

Figure 5
Approximations To Expected Stress Distributions

point due to a load of unit magnitude is known, the displacement at that point due to a similar load of any magnitude is equal to the displacement due to the unit loading times the magnitude of the loading. This can be written as:

$$WN(I,J) = P(J)*U1(I,J) \qquad (2.2)$$

$$WS(I,J) = Q(J)*U2(I,J) \qquad (2.3)$$

$$VN(I,J) = P(J)*U3(I,J) \qquad (2.4)$$

and $$VS(I,J) = Q(J)*U4(I,J) \qquad (2.5)$$

where WN(I,J) is the displacement in the normal direction at collocation point I, radius R(I) from the center, due to a normal disk load of magnitude P(J) and radius RD(J). WS(I,J) is the displacement in the normal direction at collocation point I due to a shear disk load of magnitude Q(J) and radius RD(J). VN(I,J) is the displacement in the radial direction at collocation point I due to a normal disk load of magnitude P(J) and radius RD(J). VS(I,J) is the displacement in the radial direction at collocation point I due to a shear disk load of magnitude Q(J) and radius RD(J). U1(I,J) is the displacement in the normal direction at collocation point I due to a normal disk load of radius RD(J) and unit magnitude. U2(I,J) is the displacement in the normal direction at collocation point I

due to a shear disk load of radius RD(J) and unit magnitude. U3(I,J) is the displacement in the radial direction at collocation point I due to a normal disk load of radius RD(J) and unit magnitude. U4(I,J) is the displacement in the radial direction at collocation point I due to a shear disk load of radius RD(J) and unit magnitude.

The total displacements at a collocation point are given by:

$$W(I) = \sum_{J=1}^{N} P(J)*U1(I,J) + \sum_{J=1}^{N} Q(J)*U2(I,J) \qquad (2.6)$$

and

$$V(I) = \sum_{J=1}^{N} P(J)*U3(I,J) + \sum_{J=1}^{N} Q(J)*U4(I,J) \qquad (2.7)$$

where W(I) and V(I) are the total displacements in the normal and radial directions respectively.

2.3 Approximating The Functions U1(I,J), U2(I,J), U3(I,J) And U4(I,J)

The functions U1(I,J), U2(I,J), U3(I,J) and U4(I,J) can be derived in functional form so that their values can be found for any combination of R(I) and RD(J). To evaluate the functional form of U1(I,J), U2(I,J), U3(I,J) and U4(I,J) the equilibrium equations for an elastic half-space subjected to a point load applied at the surface are

used. The appropriate equations are given in Landau and Lifshitz (8) and can be found in Appendix A. These equations are given in Cartesian coordinates and express the total displacements of any point in a half-space subjected to a point load applied at the surface. The equations can be simplified to give the displacements of points on the surface of the half-space by setting Z = 0, which results in the following set of equations:

```
UX = K1*FZ*X/R**2+K2*FX/R+K3*X*(FX*X+FY*Y)/R**3      (2.8)

UY = K1*FZ*Y/R**2+K2*FY/R+K3*Y*(FX*X+FY*Y)/R**3      (2.9)

UZ = K2*FZ/R - K1*(FX*X + FY*Y)/R**2                 (2.10)
```

where

```
K1 = -(1 + S)*(1 - 2*S)/(2*PI*E)                     (2.11)

K2 = (1 - S**2)/(PI*E)                               (2.12)

K3 = S*(1 + S)/(PI*E)                                (2.13)
```

and where S is Poisson's ratio, E is Young's modulus, PI = π, R = SQRT(X*X + Y*Y), FX, FY and FZ are the x, y and z components of the point load applied at the load applied at the origin, UX, UY and UZ are the x, y and z components of displacement and X, Y and Z are the coordinates of the point being considered. Since those equations are written for Z = 0, Z does not appear in these equations.

Equations 2.8, 2.9 and 2.10 can be rewritten as

UX = K2*UXX1*FX + K3*UXX2*FX + K3*UXY*FY + K1*UXZ*FZ (2.14)

UY = K2*UYY1*FY + K3*UYY2*FY + K3*UYX*FX + K1*UYZ*FZ (2.15)

UZ = K2*UZZ*FZ - K1*UZX*FX - K1*UZY*FY (2.16)

where

UXX1 = 1/R (2.17)

UXX2 = X**2/R**3 (2.18)

UXY = X*Y/R**3 (2.19)

UXZ = X/R**2 (2.20)

UYX = X*Y/R**3 (2.21)

UYY1 = 1/R (2.22)

UYY2 = Y**2/R**3 (2.23)

UYZ = Y/R**2 (2.24)

UZX = X/R**2 (2.25)

UZY = Y/R**2 (2.26)

UZZ = 1/R (2.27)

Equations 2.14, 2.15 and 2.16 give the displacements of a point on the surface due to a point load. In order to find the displacements of the surface due to a stress distribution $\underline{S(X,Y)}$, the stress distribution is put into vector form.

$$\underline{S(X,Y)} = SX(X,Y)\underline{i} + SY(X,Y)\underline{j} + SZ(X,Y)\underline{k} \quad (2.28)$$

where $\underline{i}$, $\underline{j}$ and $\underline{k}$ are the unit vectors in the x, y and z directions, respectively. By replacing FX, FY and FZ by

SX(X,Y), SY(X,Y) and SZ(X,Y) in equations 2.14, 2.15 and 2.16 and integrating over the entire region where the stress distribution acts these equations become:

$$UX = K1*\int UXZ*SZ(X,Y)d\Omega + K2*\int UXX1*SX(X,Y)d\Omega + K3*\int UXX2*SX(X,Y)d\Omega + K3*\int UXY*SY(X,Y)d\Omega \quad (2.29)$$

$$UY = K1*\int UYZ*SZ(X,Y)d\Omega + K2*\int UYY1*SY(X,Y)d\Omega + K3*\int UYY2*SY(X,Y)d\Omega + K3*\int UYX*SX(X,Y)d\Omega \quad (2.30)$$

$$UZ = K2*\int UZZ*SZ(X,Y)d\Omega - K1*\int UZX*SX(X,Y)d\Omega - K1*\int UZY*SY(X,Y)d\Omega \quad (2.31)$$

where Ω is the entire region over which the stress distribution acts.

Since the shear stress distribution is to be approximated by the loading shown in Figure 4, SX(X,Y) and SY(X,Y) can be replaced by SR*cosθ and SR*sinθ, where SR = R/RD and θ = arctan(X/Y) as in Figure 6. This yeilds

$$SX(X,Y) = (R/RD)*(X/R) = X/RD \quad (2.32)$$

$$SY(X,Y) = (R/RD)*(Y/R) = Y/RD \quad (2.33)$$

Similarly SZ(X,Y) can be replaced by a constant value of unity so that

$$SZ(X,Y) = 1 \quad (2.34)$$

The displacements UX, UY and UZ in equations 2.29, 2.30 and 2.31 are those of points along the radial line corresponding to the X axis (see Figure 3). It can be seen

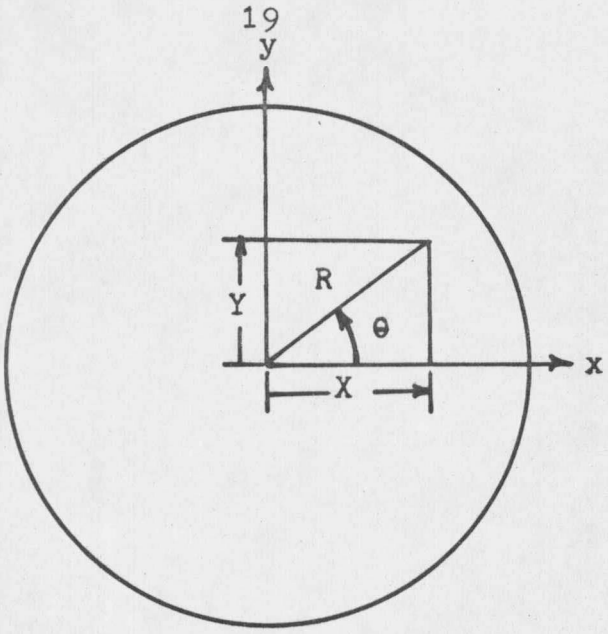

$X = R*\cos\theta;\ Y = R*\sin\theta$

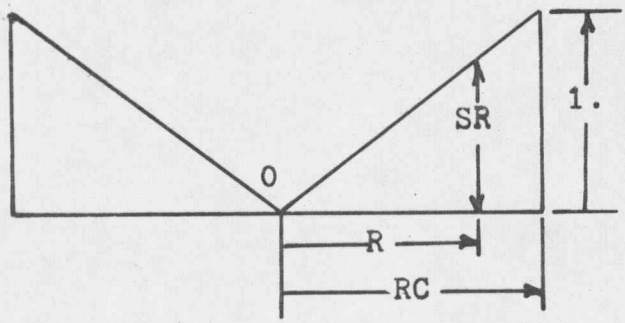

$SX = SR*\cos\theta = (R/RD)*(X/R) = X/RD$
$SY = SR*\sin\theta = (R/RD)*(Y/R) = Y/RD$

Figure 6
SX And SY In Terms Of X, Y And R

that the radial displacements along this line are the same as UY and from symmetry must be zero. Similarly the radial displacements are the same as UX. The normal displacements are UZ.

Therefore

$$U1 = K2*\int UZZ*SZ(X,Y)\,d\Omega \tag{2.35}$$

$$U2 = -K1*\int UZX*SX(X,Y)\,d\Omega \quad -K1*\int UZY*SY(X,Y)\,d\Omega \tag{2.36}$$

$$U3 = K1*\int UXZ*SZ(X,Y)\,d\Omega \tag{2.37}$$

$$U4 = K2*\int UXX1*SX(X,Y)\,d\Omega \quad + K3*\int UXX2*SX(X,Y)\,d\Omega + K3*\int UXY*SY(X,Y)\,d\Omega \tag{2.38}$$

Of the above integrals only

$$\int UZZ*SZ(X,Y)\,d\Omega$$

results in a commonly used function. This integral results in elliptic functions.

The integrals in equations 2.29, 2.30 and 2.31 were evaluated numerically (see Appendix B for details). Plots of the values obtained for the integrals for various ratios of R(I) to RD(J) are shown in Figures 7, 8, 9 and 10. No plots for the y displacements are shown since they are all zero as is expected due to symmetry. Also the sum of

$$\int UXX2*SX(X,Y)\,d\Omega \quad + \int UXY*SY(X,Y)\,d\Omega$$

is equal to zero. Since the sum

$$\int UZX*SX(X,Y)\,d\Omega \quad + \int UZY*SY(X,Y)\,d\Omega$$

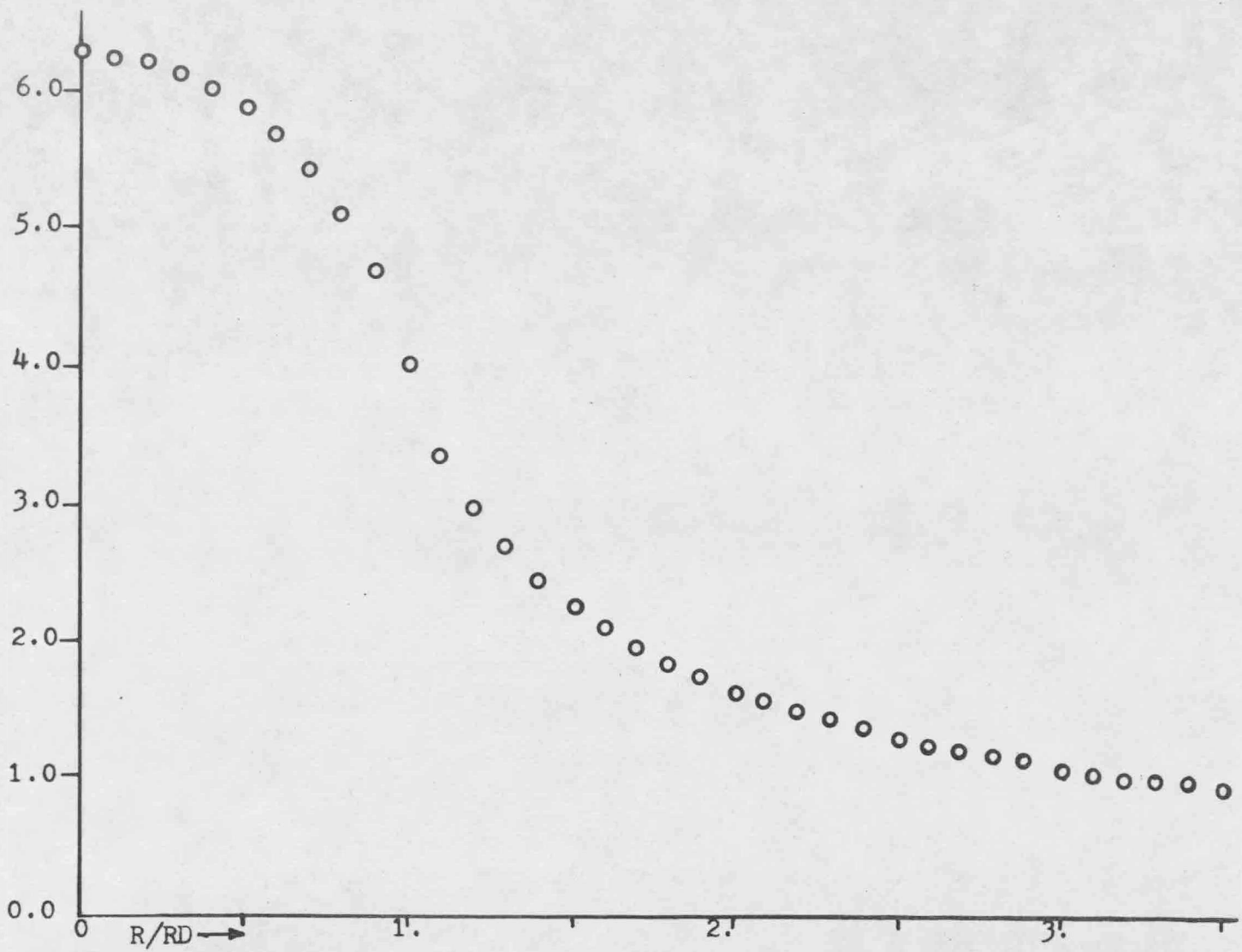

Figure 7 Values Obtained For UZZ By Numerical Integration

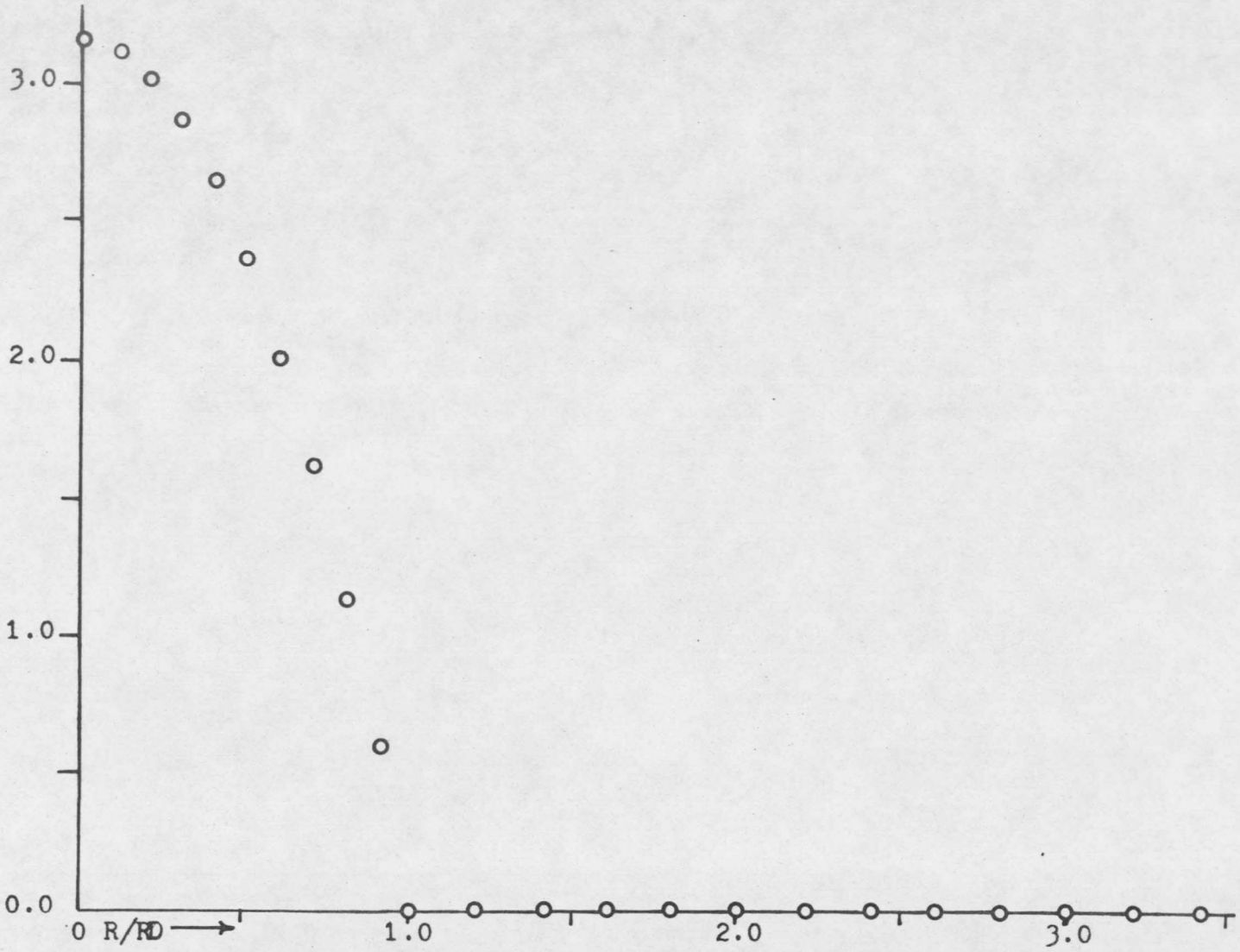

Figure 8 Values Obtained For UZX + UZY By Numerical Integration

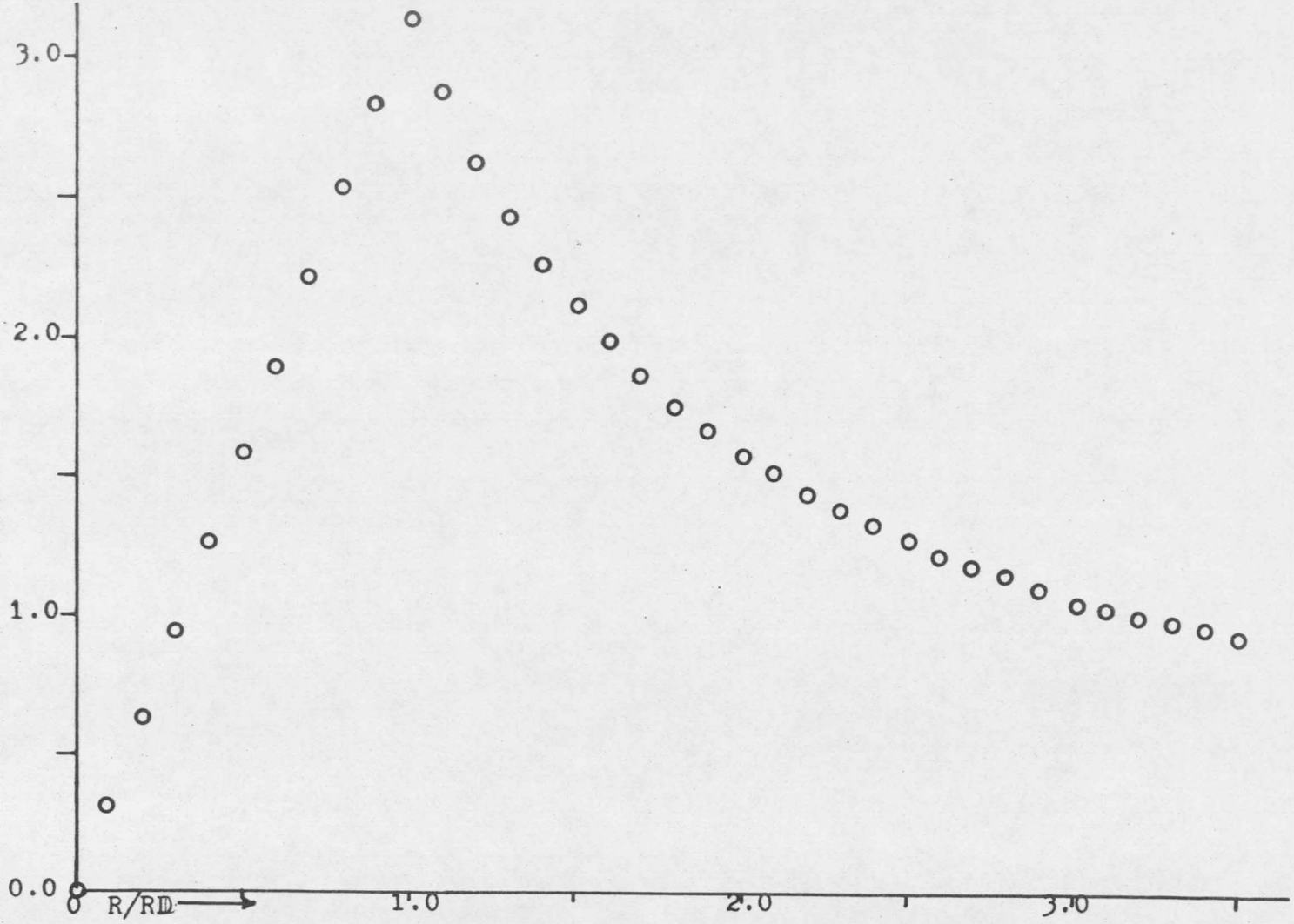

Figure 9 Values Obtained For UXZ By Numerical Integration

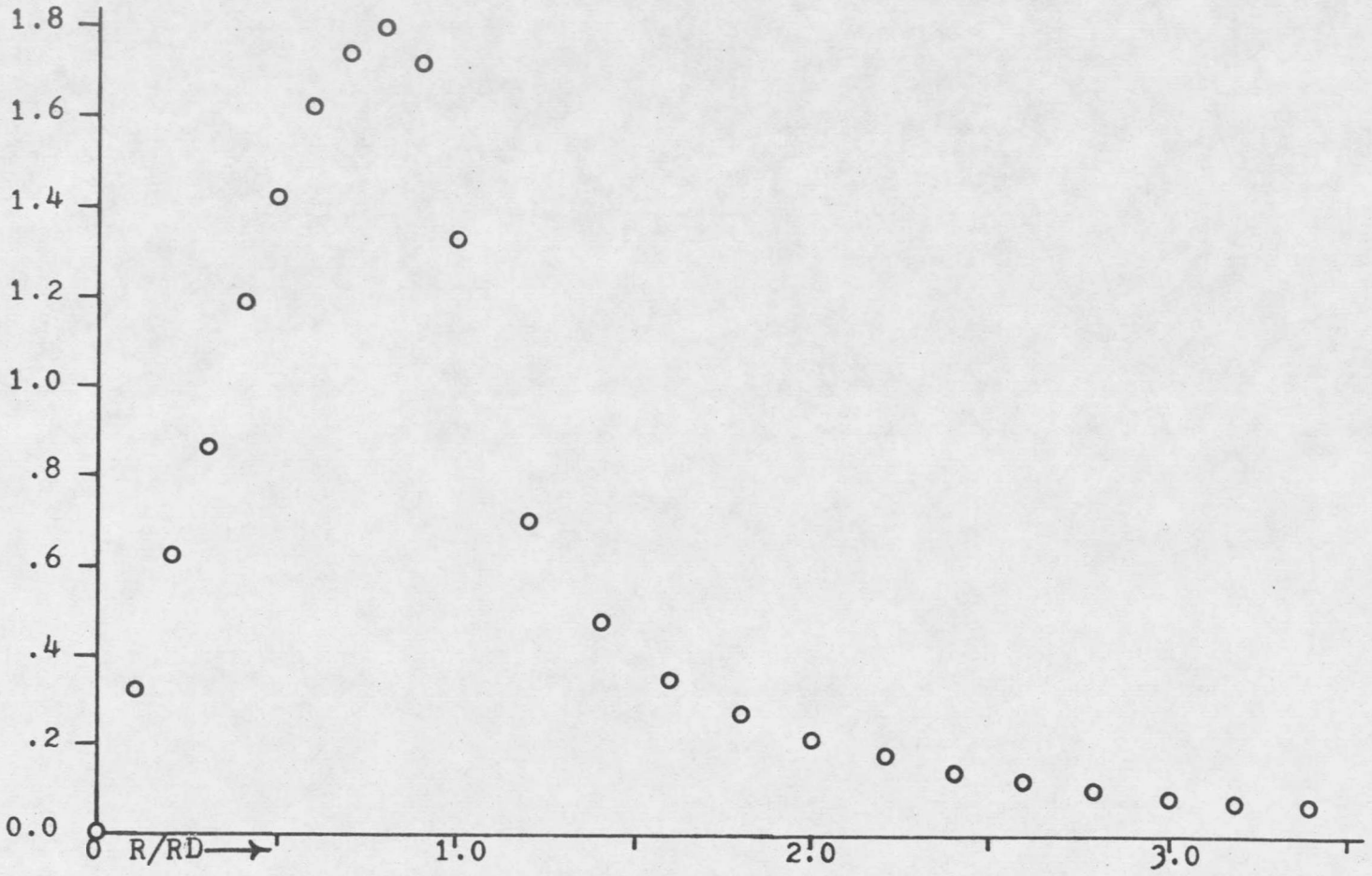

Figure 10 Values Obtained For UXX1 By Numerical Integration

is equal to zero outside the contact region these two integrals are combined and shown plotted in Figure 8.

The values obtained for

$$\int UZZ^{*}SZ(X,Y)\,d\Omega$$

by numerical integration are very close to the values tabulated for this elliptic integral. The maximum error for the values inside the contact region is 0.07 percent and only five of the thirty values outside the contact region exceed 1.0 percent error. The errors here were used as a check on the numerical integration methods. Values for the errors for each point are included in Appendix B together with the errors between the computed values and equations used to approximate the remainder of the integrals.

Approximations to the remaining integrals were obtained and resulted in the following:

	$R \leq RD$	$R > RD$	
U1/K2 =	4*R*Ė;	4*R*(Ė-K*(1-(RD/R)**2))	(2.38)
U2/K1 ≈	RD*PI*(1-(R/RD)**2);	0	(2.39)
U3/K1 ≈	PI*R;	PI*RD**2/R	(2.40)
U4/K2 ≈	4/3*R*Ė**2;	4/PI*R**2/RD*(Ė-K*(1-(RD/R)**2)**2	(2.41)

where $\dot{E}$ = elliptic integral of the first kind

K = elliptic integral of the second kind

RD = radius of the disk load

R = radius of the collocation point

Of all these equations only the values given for U1 are exact. The values obtained from the equations approximating U2 are all within 0.34 percent of the values obtained from the numerical integration. The values for the approximation to U3 are within 0.27 percent of the numerical integration values inside the contact region and within 4.0 percent outside the contact region. The values for the approximation to U4 are all within 4.6 percent of the computed values. Attempts to improve on the approximations did not improve the results of the general stress calculation method.

2.4 The Numerical Method Used For Solving The Simultaneous Equations

The formulation of the problem has resulted in 2 N equations (2.6 and 2.7) in the 2 N unknowns, namely the magnitudes of the N normal disk loadings and the N shear disk loadings. All that remains to solve the problem for known displacements is to find a solution to these 2 N simultaneous equations. However, there is some difficulty

in solving these equations. They are ill posed in the sense that solutions are hard or even impossible to obtain by such methods as Gaussean elimination if N is larger than four or five even if double precision on a computer, which uses sixteen digits, is used. The computer that was used for all computations is the Xerox Sigma 7.

An alternative method that works for N about twenty is the Gauss-Seidel iteration procedure using a subroutine from Carnahan (3). Even this latter method does not work if the collocation points are picked improperly. The coefficient matrix that is obtained is very nearly singular and it is possible that small variations in any one coefficient could cause meanless results to be obtained. Since this is the case, and since this was the best of the several methods attempted, a test case using a known stress distribution was solved in order to establish some confidence in this latter method.

2.5 Test Cases Using Known Displacements

The method described in section 2.4 can be used to find the surface stresses if the surface displacements are known. To test this method of solution a set of surface displacements corresponding to a known stress distribution was used for different test cases. The first of these used a stress distribution similar to the expected stress distribution between the rigid sphere and the elastic half-space. The second test case used the normal displacements from the Hertzian contact problem and found only the normal stress distribution.

The expected normal stress distribution between the rigid sphere and the elastic half-space is similar to the Hetzian stress distribution in both magnitude and shape. The stress distribution used was the first quarter cycle of a cosine wave with its maximum magnitude equal to the maximum magnitude of the Hertzian stress for the friction-less contact problem with the same contact radius. The expected shear stress distribution has a zero value at the center and outside edge of the contact region and has its maximum somewhere in between. The maximum value of the shear stress is expected to be between zero and fifty percent of the maximum normal stress. The stress

distribution used was the first half cycle of a sine wave with a maximum magnitude equal to thirty percent of the maximum normal stress.

To calculate the displacements of the half-space surface due to these stress distributions a numerical integration similar to the one used to find U1, U2, U3 and U4 was done. The program used is listed in Appendix C. Using the displacements obtained from this program the methods for finding the stresses that were developed in sections 2.3, 2.4 and 2.5 were used to find the stress distributions. The results obtained for this test case are shown in Figures 11 and 12. As can be seen from Figure 11 the normal stress distribution was approximated very well. If the value of the 'known' normal stress at the mid-point of each region is compared to the value of the approximation to the normal stress at this point, the values are within one percent of each other except at the outermost region. As can be seen from Figure 12 the shear stress was also predicted fairly well. Due to the jagged nature of the approximation it is difficult to compare it to the 'known' shear stress distribution numerically. It can be seen that the shear stress was under predicted near the center of the region and over predicted near the

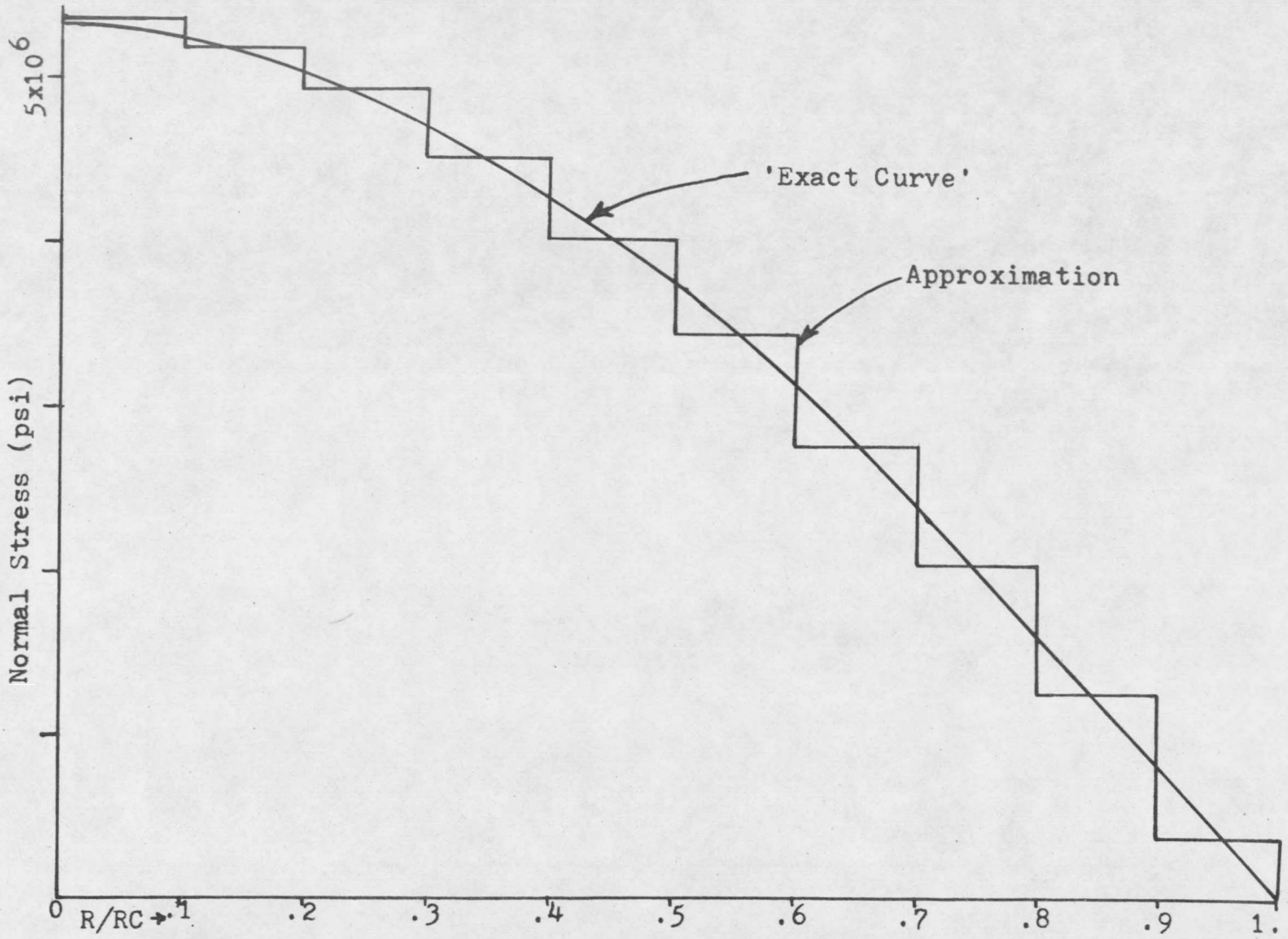

Figure 11 Approximation To Known Surface Normal Stress

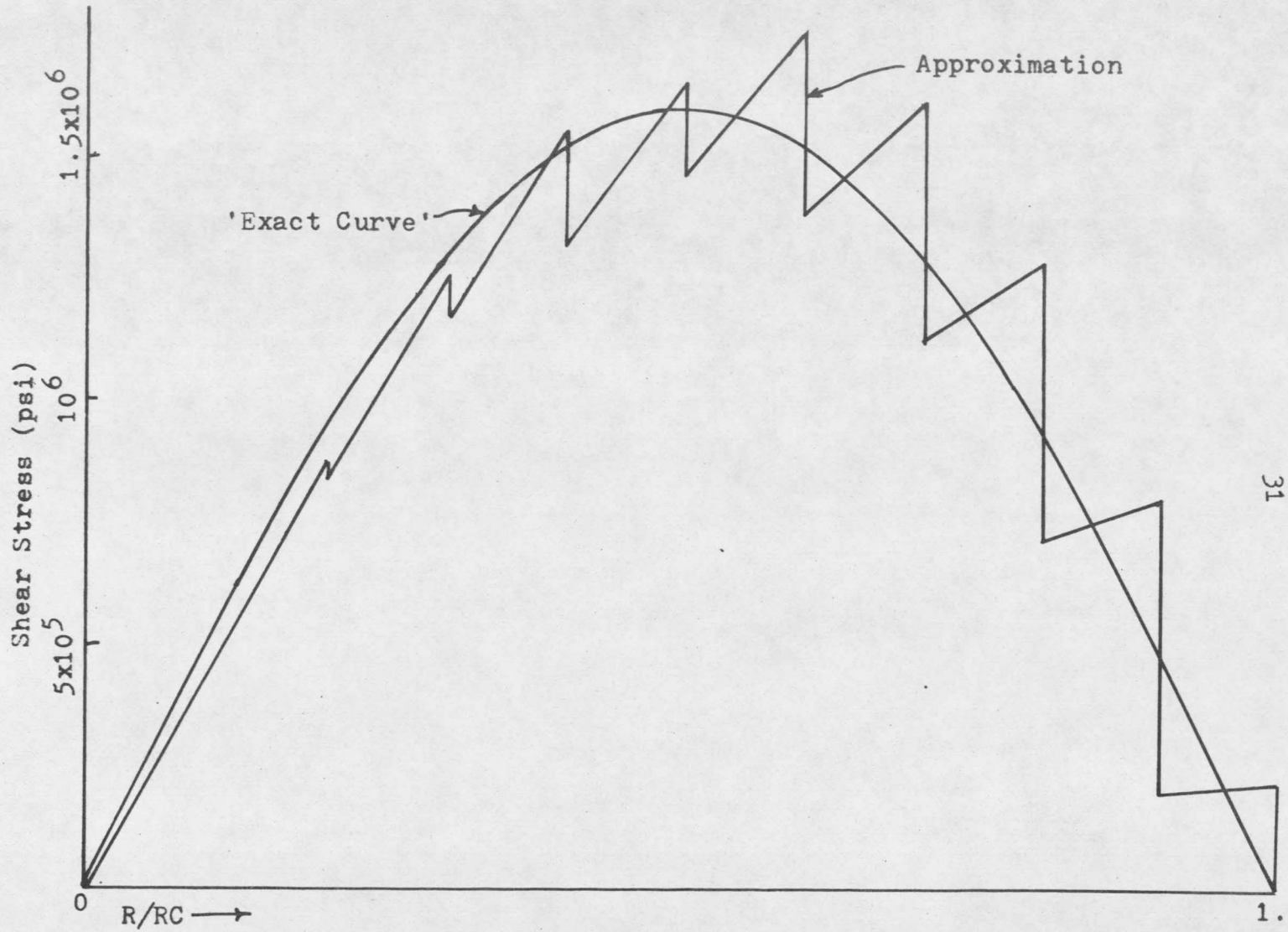

Figure 12 Approximation To Known Surface Shear Stress

outside edge.

The second test case that was tried was the Hertzian contact problem. The particular geometry that was used was a sphere contacting a half-space. In this case only the normal stresses were included. The results are shown in Figure 13. The approximation was very good with a maximum error of only 2.6 percent. Using these two test cases as a check supplies the needed confidence to be reasonably sure that if the displacements can be found the stresses will be closely approximated.

2.6 The Method For Surface Displacement Determination

Now that it is possible to closely approximate the surface stresses if the surface displacements are known, an additional requirement is a method to predict the surface displacements accurately. There are some difficulties in finding both the normal and radial displacements. The total normal displacements within the contact region can be written as:

$$W = APP - F \tag{2.42}$$

where W is the total displacement at a point, F is the value of the profile function at the point and APP is the approach of the two bodies. The function F is given by equation 2.1. For two elastic bodies the approach is

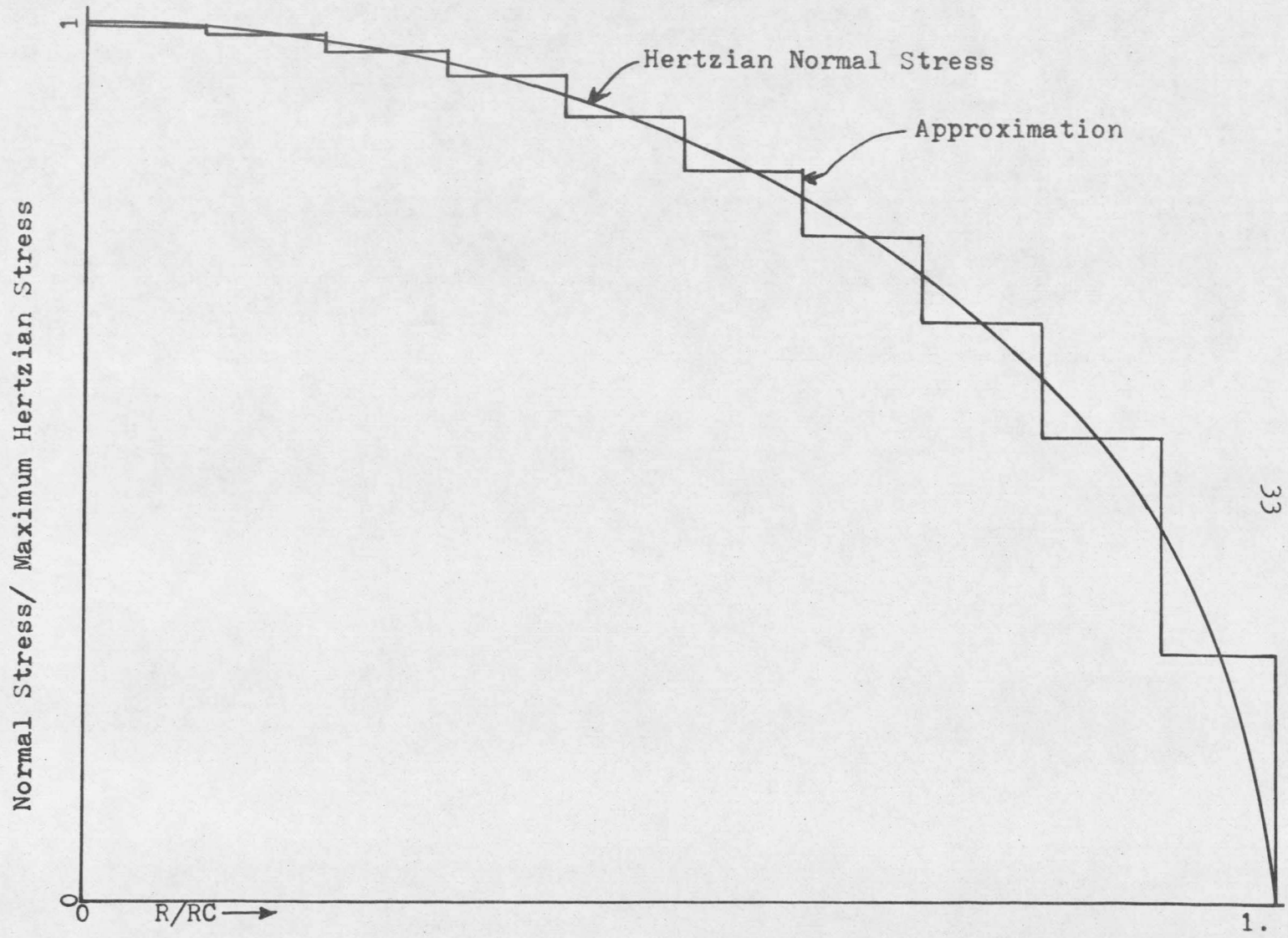

Figure 13 Approximation To Known Hertzian Normal Stress

defined as the relative approach of two points, one of which is in each body and both are far removed from the contact region. Since the sphere is rigid the entire normal displacement will take place in the half-space and the approach is equal to the normal displacement at the origin of the half-space as shown if Figure 2. The profile function is known, therefore all that remains to be found to solve for the normal displacements is the approach. Theoretically it is simple to express the approach in terms of the other unknowns in the problem. There are already 2 N equations in terms of the 2 N + 1 unknowns. The unknowns are the approach and the N magnitudes of the normal disks and the N magnitudes of the shear disks. If one more equation is written relating the normal displacement at one more point to the approach and the 2 N disk magnitudes, there would be 2 N + 1 equations in 2 N + 1 unknowns. However, this method yeilded equations which were not solvable numerically. Attempts to write the last equation using normal displacements at several different points failed to help. Attempts to use the methods developed by Singh (15) did not help. Since it was not possible to solve for the approach using this method, another method was developed which approximated the

approach.

The normal displacements caused by a unit disk of shear stress are less than fifty percent of the normal displacements caused by a unit disk of normal stress. This fact and the fact that the maximum magnitude of the shear stress is expected to be less than twenty five percent of the maximum magnitude of the normal stress combine to lead to the approximation of about twelve percent and probably less than five or ten percent error if only the normal stress is used to approximate the approach. Using this rational it is reasonable to approximate the load versus approach relationship by using the equations of Hertz. The Hertzian load versus approach relationship is

```
APP = ((3*PI*P*K1/4)**2/R2)**(1/3)                    (2.43)
```

where P = total load and

```
K1 = (1 - S**2)/(PI*E)
```

This equation is then used to approximate the approach in the solution technique developed.

The steps in the procedure are (1) to approximate the approach using equation 2.43, (2) to calculate the stresses and the total load and (3) to use the Hertzian load versus approach relationship to iterate to a new value for the

approach. The equation used for the new approximation of the approach is

APP = R2*R2/R1*(6*HLOAD**(2/3) - 5*HLOAD1**(2/3)) (2.44)

where R2*R2/R1 = Hertzian approach for the same contact radius

HLOAD = load/Hertzian load for the same contact radius

= 3*P*R1*PI*K1/(4*R2**3)

HLOAD1 = HLOAD from the previous step

Equation 2.44 was used rather than equation 2.43 to get a new approach because of the more rapid convergence. By using equation 2.44 the method converges in four or five iterations instead of forty or fifty iterations required with direct substitution. Now that it is possible to calculate the approach, the displacements in the normal direction can be considered as known.

Next a method is developed to calculate the radial displacements. Consider what actually takes place as a rigid sphere is pushed into an elastic half-space. The sphere and half-space are initially in contact at only one point. As a load is applied a circular contact region develops and points on the surface of the half-space are pushed away from the origin in the radial direction.

Points both inside and outside the contact region are displaced, although points in the contact region tend to be held back because of friction between the surfaces. Depending on the coefficient of friction and the ratio of shear stress to normal stress, the points in the contact region either stick to the sphere or slip with respect to the sphere. This continuous process of sticking and slipping must be broken down into finite steps in order to use the collocation method.

In each step the surface displacements and stresses must be approximated. In addition the shear stresses must be limited to their proper values. The method developed initially considers the two bodies in contact at only one point. Next the sphere is moved toward the half-space a small distance until the radius of contact is R2, during which motion the radial displacements are taken to be zero. With the given contact radius R2 the approach is found by using the iteration procedure given in this section. Using the calculated value for the approach the normal and shear stresses are calculated. The values of the shear stresses at the collocation points are limited to the coefficient of friction times the normal stress at the same collocation point stress is equivalent to letting the

surface slip in regions where there should be slippage. With the limited shear stresses in the next step the radial displacements are calculated at the collocation points. This completes the first step.

For the next step the contact radius is increased to a new value R2 + R2STEP, where R2STEP is the amount that the contact radius is increased. This is equivalent to pushing the sphere further into the half-space. Everything proceeds in the same manner as in the first step except that the radial displacements are calculated using the previous step's stress distributions. After the approach is found and the stresses calculated and limited, the process is repeated until there is no appreciable change in the dimensionless form of the load, approach, stresses and displacements. This takes about fifty steps.

The dimensionless forms are based on the Hertzian quantities for the same contact radius and are as follows:

PSTAR = P/Hertzian load = P*R1*3/4*(1-S.**2)/(R2**3*E) (2.45)

APPSTAR = APP/Hertzian approach =APP*R1/R2**2 (2.46)

STRESSSTAR = STRESS/Max Hertzian Stress = STRESS/PO (2.47)

DISPSTAR=DISP/Hertzian Approach = DISP*R1/R2**2 (2.48)

The dimensionless quantities are based on the Hertzian

values since the Hertzian results can be expressed in terms of only the elastic properties and the contact radius. Changes in the contact radius change the relative magnitudes of the stresses and displacements, but do not change the shapes of the stress and displacement curves. Including the effects of friction changes the shapes of these curves but the curves for a specific coefficient of friction are similar.

The methods and procedures that have been developed were combined in the computer program that is listed in Appendix D. This program was run several times using different coefficients of friction to obtain the effects of friction on the various parameters involved in the contact problem.

Chapter 3

RESULTS AND DISCUSSION

3.1 The Coefficient Of Friction Range

The methods developed in the previous chapter and listed in the computer program of Appendix D were used to examine the effects of varying the coefficient of friction on the contact stresses. The coefficients of friction used were 0.05, 0.10, 0.20 and infinity. These friction coefficients cover the range of sliding coefficients of friction found in contact between metals. Values between 0.20 and infinity were not used because a coefficient of friction of above about 0.25 results in no slippage between the sphere and half-space. In actuality since the normal stress goes to zero at the outside edge of the contact region it appears that if the coefficient of friction is finite some slipping will occur near the outside edge. However, since the methods used approximate the stresses by a series of disk loads, the values of the normal and shear stresses are approximated such that a value of 0.25 for the coefficient of friction results in no slippage. The results that were obtained are listed in Tables 1 to 5 and are plotted in Figures 14 to 21. The values for the stresses in Tables 1 and 2 have been divided by the maximum Hertzian

stress associated with the same contact radius. Similarly the radial displacements have been divided by the Hertzian approach associated with the same contact radius to put them into dimensionless form. The value used for Young's modulus was 30,000,000 psi and the value for Poisson's ratio was 0.3. These are the values associated with steel.

3.2 Effects Of The Coefficient Of Friction On The Surface Normal Stresses

The values obtained for the dimensionless normal stresses at each of the collocation points are listed in Table 1. The maximum magnitudes of the normal stresses are 8.5 to 18.6 percent higher than the maximum Hertzian stress associated with the same contact region. The larger the coefficient of friction, the larger the magnitude of the normal stress in any one region. If the normal stresses are compared to the Hertzian stress associated with the same load, instead of the same contact radius, the maximum magnitudes are from 3.2 to 8.5 percent higher than the maximum Hertzian stress. The values non-dimensionalized with respect to the Hertzian values associated with the same load are given in Table 5.

The values from Table 1 are plotted in Figure 14. The normal stress curves are similar in both shape and magnitude

Table 1 Normal Stresses At The Collocation Points Nondimensionalized With Respect To The Maximum Hertzian Stress Associated With The Same Contact Radius

Collocation Number	$\mu = \infty$	$\mu = .20$	$\mu = .10$	$\mu = .05$
1	1.186	1.168	1.118	1.085
2	1.170	1.155	1.104	1.071
3	1.143	1.132	1.081	1.046
4	1.104	1.097	1.046	1.011
5	1.055	1.048	.998	.965
6	.994	.986	.938	.908
7	.919	.911	.864	.836
8	.825	.819	.773	.745
9	.701	.702	.657	.628
10	.652	.646	.558	.496

Table 2 Shear Stresses At The Collocation Points Nondimensionalized With Respect To The Maximum Hertzian Stress Associated With The Same Contact Radius

Collocation Number	$\mu = \infty$	$\mu = .20$	$\mu = .10$	$\mu = .05$
1	-.028	-.021	-.017	-.014
2	-.072	-.050	-.039	-.033
3	-.104	-.080	-.058	-.044
4	-.127	-.111	-.075	-.049
5	-.142	-.133	-.086	-.046
6	-.155	-.142	-.088	-.045
7	-.169	-.150	-.086	-.042
8	-.179	-.152	-.077	-.037
9	-.175	-.140	-.066	-.031
10	-.102	-.125	-.056	-.025

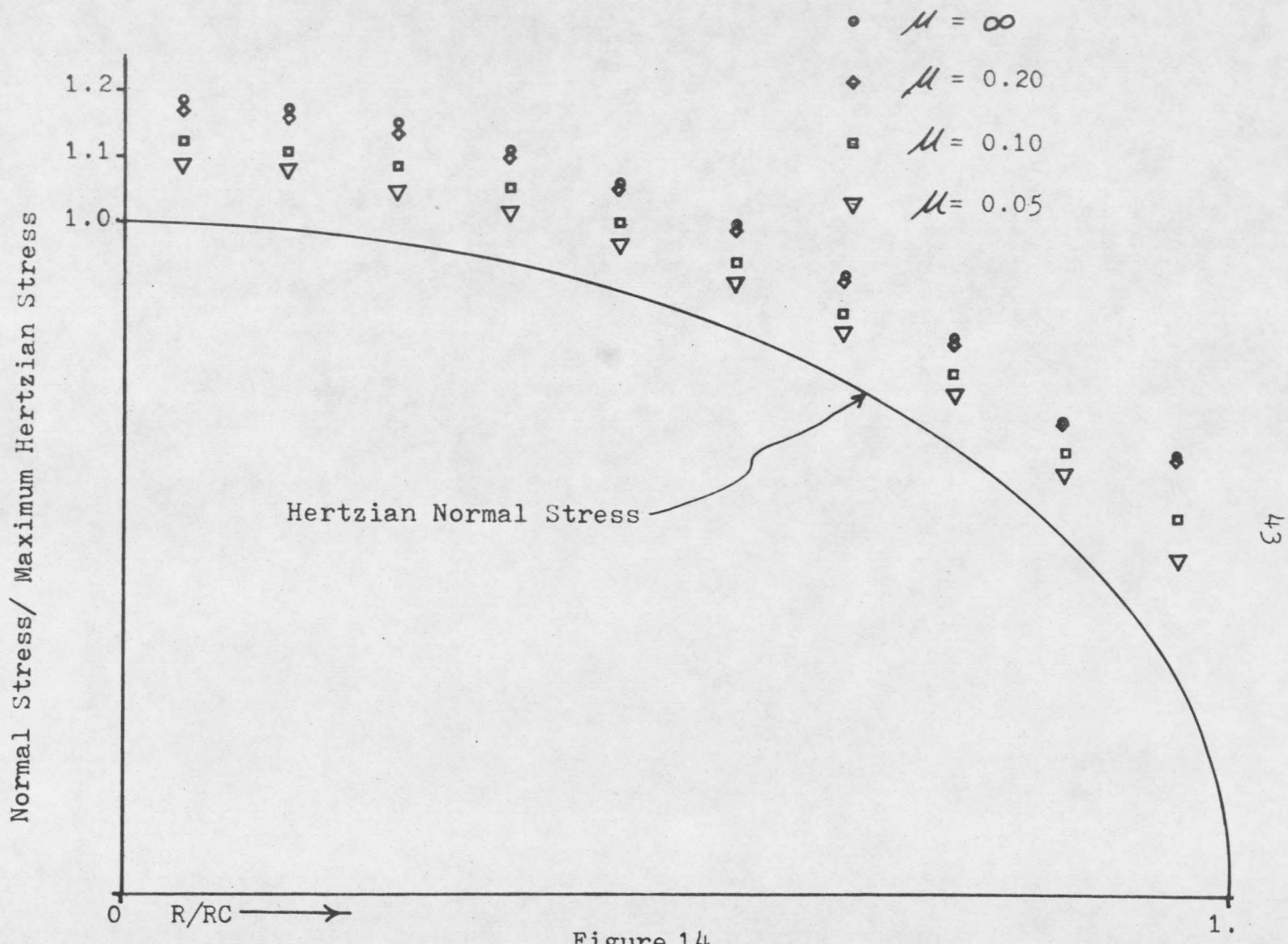

Figure 14
Effects Of Several Coefficients Of Friction On The Surface Normal Stresses At The Collocation Points

to the normal stress curves predicted by Hertz, therefore the assumption that the Hertzian load versus approach relationship could be used for the non-Hertzian problem appears to be reasonable.

For the various coefficients of friction the predicted normal stresses at the outside collocation point are from 70.7 to 124.4 percent higher than the Hertzian stress at the outside collocation point. Including friction in the problem increases the normal stress more at the outside edge than it does at the center of the contact region.

3.3 Effects Of The Coefficient Of Friction On The Surface Shear Stresses

The values obtained for the dimensionless shear stress at each of the collocation points are listed in Table 2. The shear stresses are negative because they act toward the center of the contact region and the positive shear stress was picked as away from the center. The maximum value of the shear stress is 0.179 times the maximum Hertzian stress for the same contact radius. As was expected this was for a coefficient of friction of infinity. As the coefficient of friction is decreased the magnitude of the shear stress in any one region is reduced. The values from Table 2 are plotted in Figures 15 to 18. In Figure 19 the shear stress

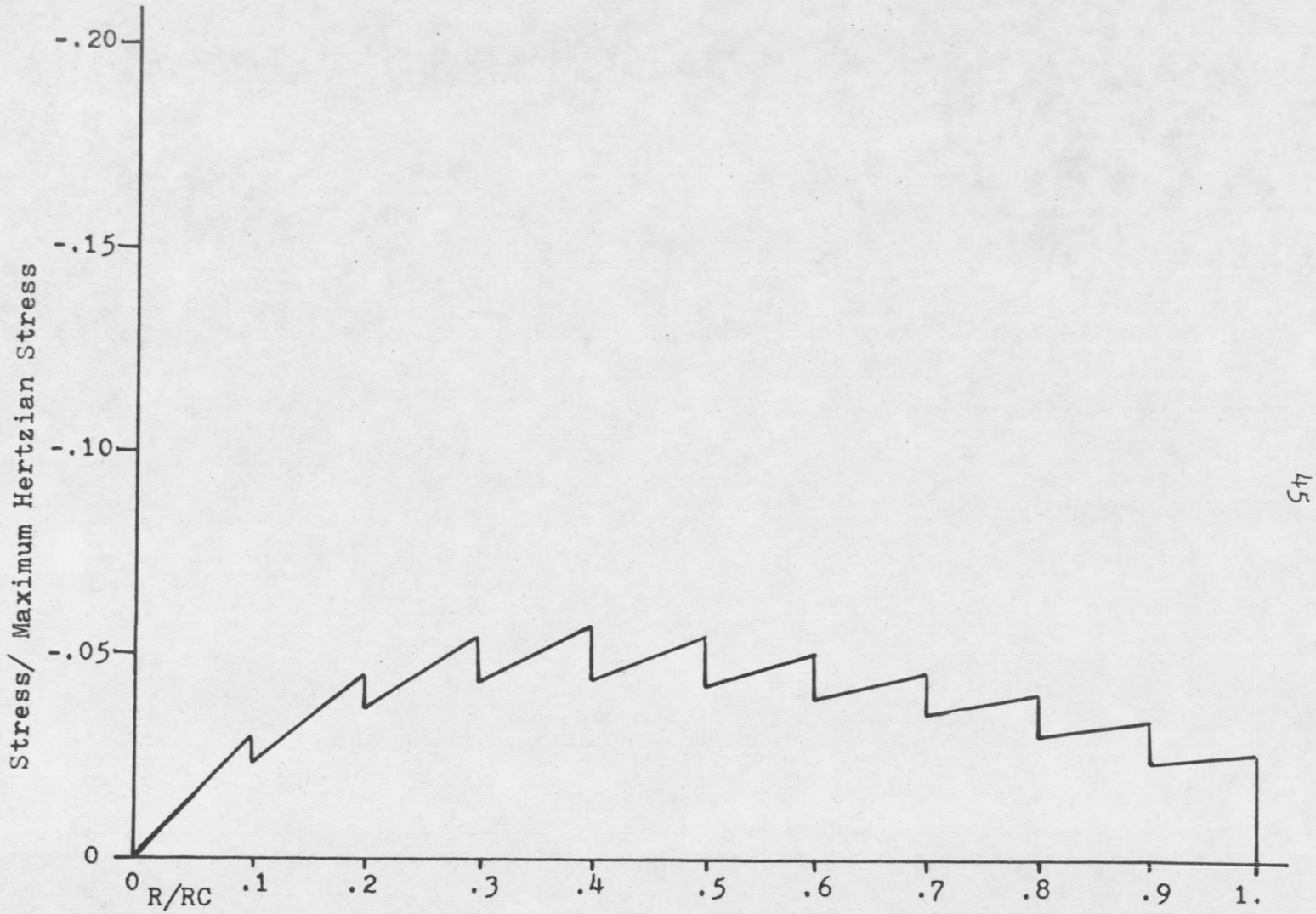

Figure 15
Approximation To Surface Shear Stress For μ = 0.05

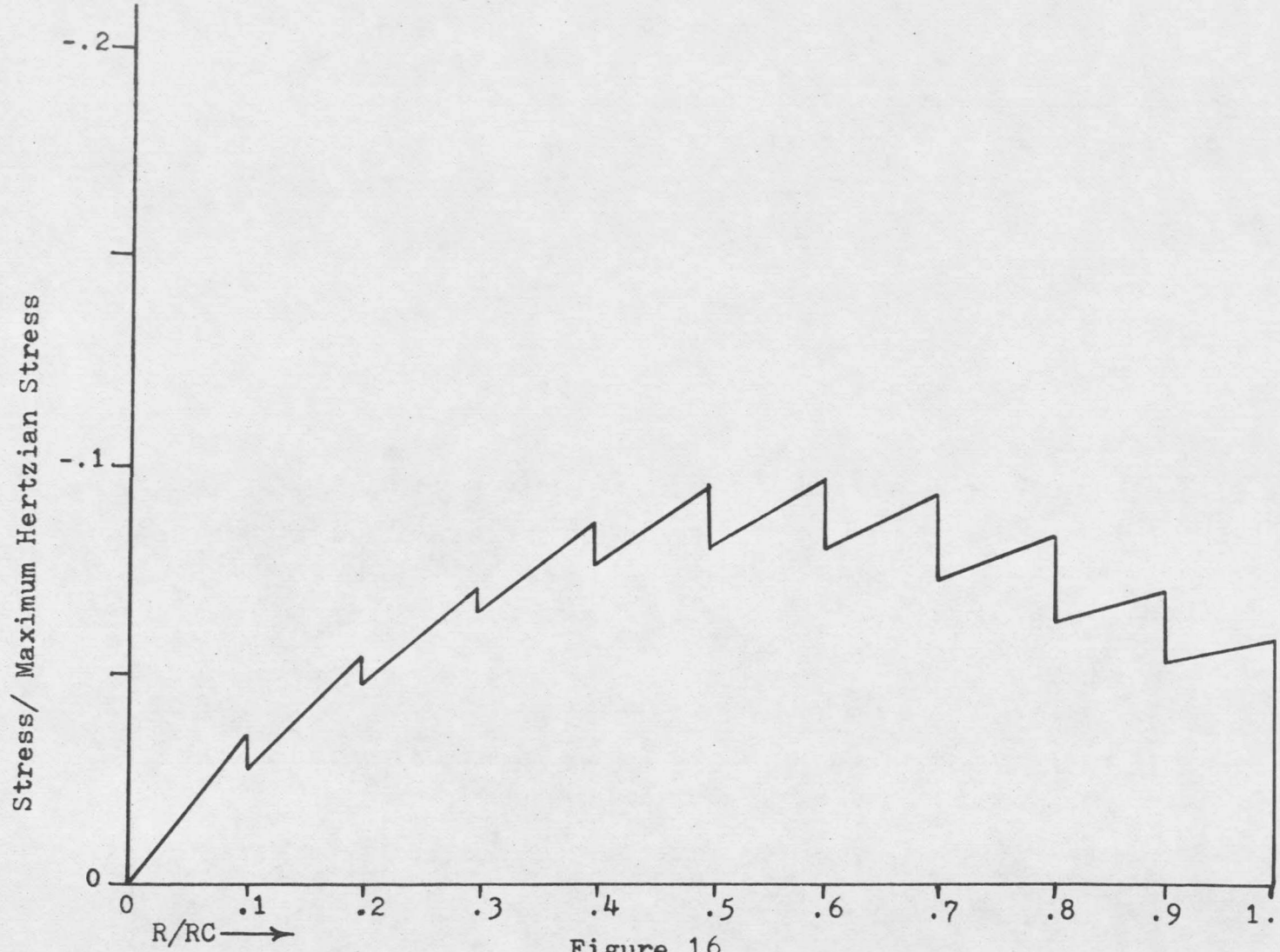

Figure 16
Approximation To Surface Shear Stress For μ = 0.10

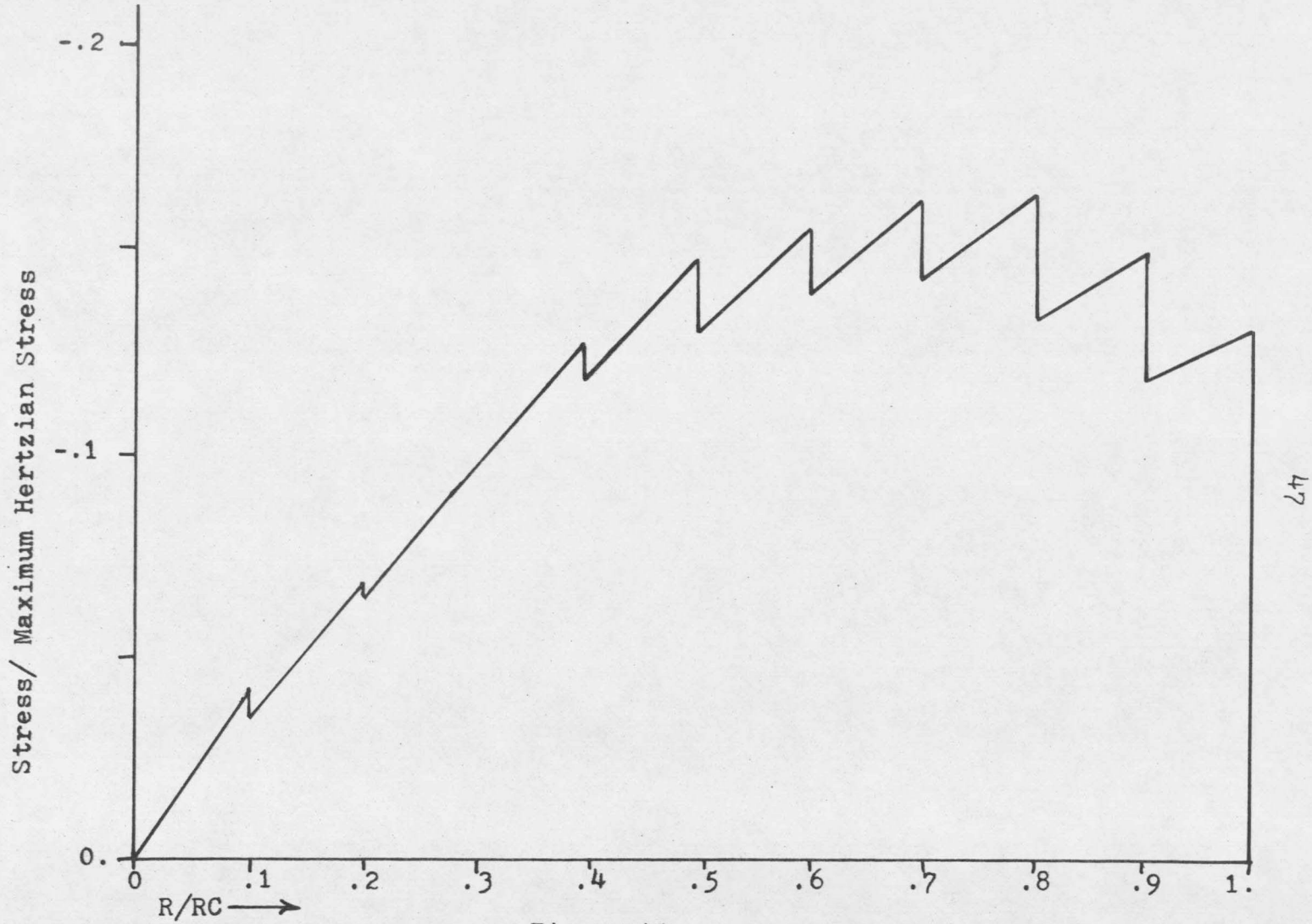

Figure 17
Approximation To The Surface Shear Stress For μ = 0.20

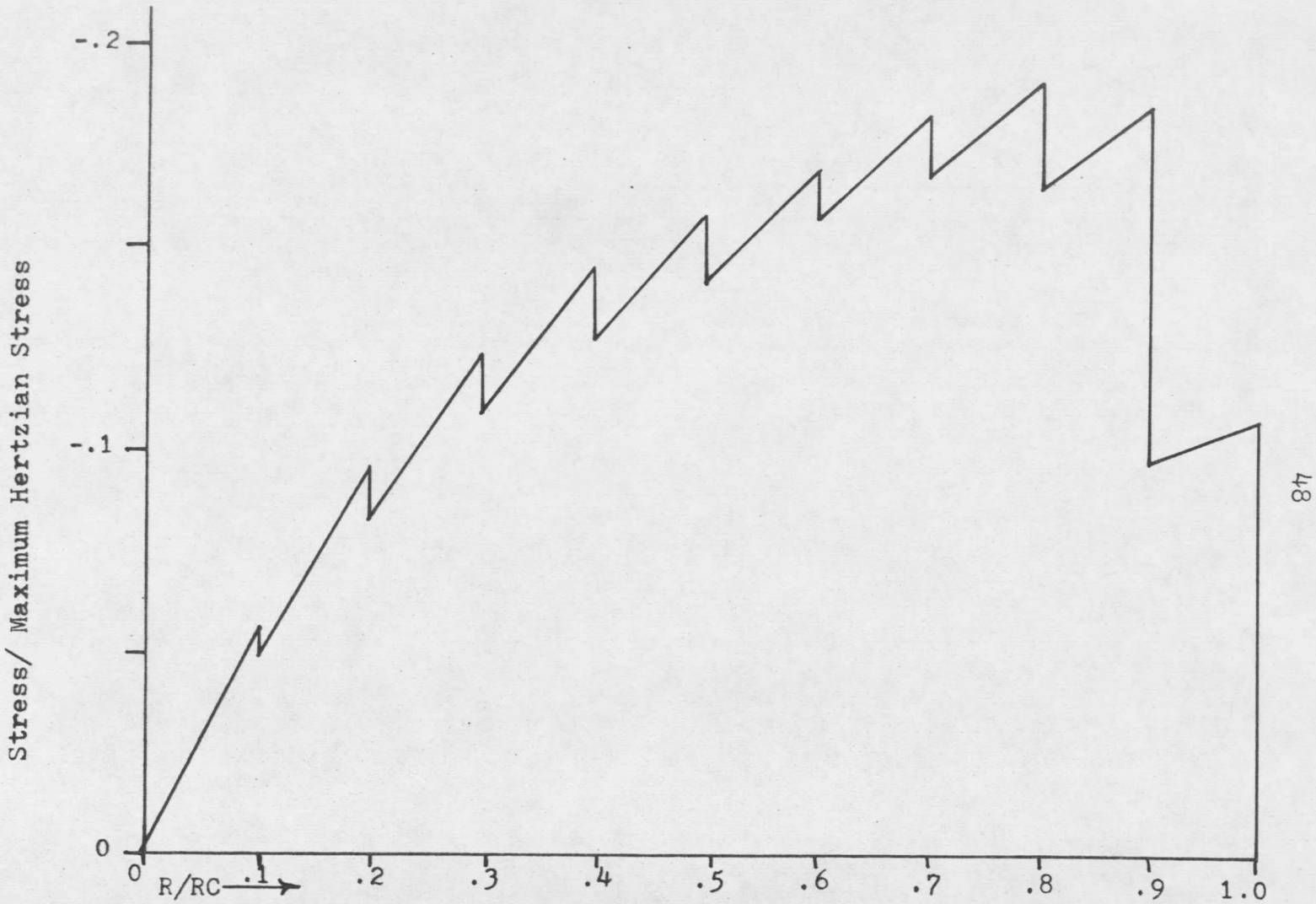

Figure 18
Approximation To The Surface Shear Stress For $\mu = \infty$

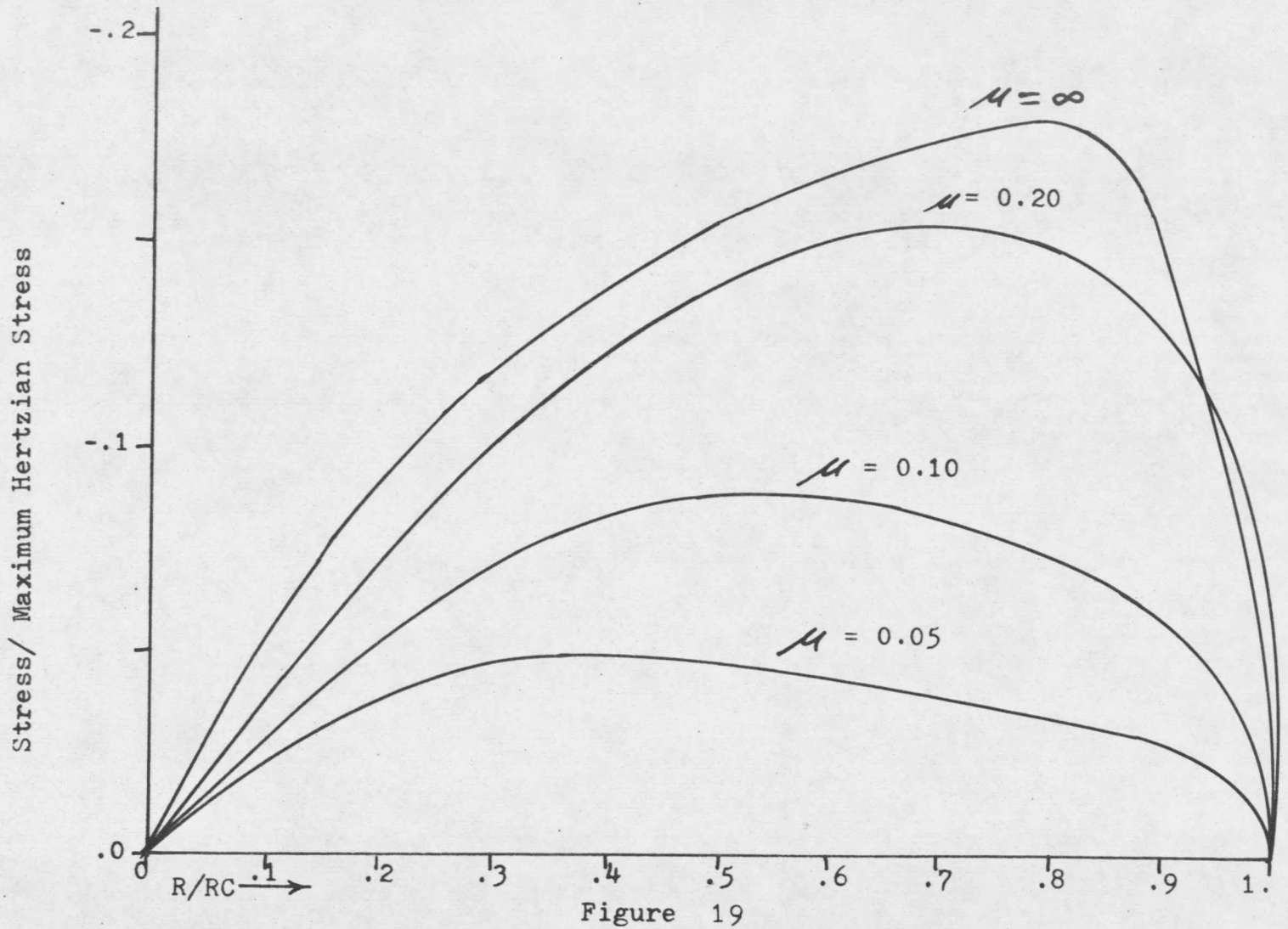

Figure 19

Effects Of Several Coefficients Of Friction On Surface Shear Stress

curves that are shown are the smooth curves that were obtained by drawing a line through the approximations to the shear stress curves at the collocation points. From Figure 19 it can be seen that the larger the coefficient of friction, the farther from the center of the contact region that the maximum value of the shear stress occurs.

Listed in Table 3 are the values of the local shear stress divided by the local normal stress at each of the collocation points. These values are plotted in Figure 20. From this figure it is possible to determine the regions of slip and stick. In those regions where the shear stress divided by the local normal stress is equal to the coefficient of friction the two bodies have slipped with respect to each other. In these regions the shear stress tended to be higher than the allowable value, so slippage took place between the sphere and the half-space. In those regions where the shear stress divided by the normal stress is less than the coefficient of friction the stresses are such that no slippage occurs and the two bodies in effect stick to each other. The radius to the slip region for a coefficient of friction of 0.20 is about 0.8 times RC, for a coefficient of friction of 0.10 it is about 0.6 times RC and for a coefficient of friction of 0.05 it is about 0.4

Table 3 Shear Stress / Normal Stress At Collocation Points For Several Coefficients Of Friction

Collocation Number	$\mu = \infty$	$\mu = .20$	$\mu = .10$	$\mu = .05$
1	-.024	-.018	-.015	-.013
2	-.061	-.044	-.035	-.030
3	-.091	-.071	-.054	-.042
4	-.115	-.101	-.072	-.048
5	-.135	-.127	-.086	-.050
6	-.156	-.144	-.094	-.050
7	-.184	-.164	-.100	-.050
8	-.217	-.186	-.100	-.050
9	-.249	-.200	-.100	-.050
10	-.157	-.193	-.100	-.050

Table 4 Radial Displacements At The Collocation Points Nondimensionalized With Respect To The Hertzian Approach For The Same Contact Radius

Collocation Number	$\mu = \infty$	$\mu = .20$	$\mu = .10$	$\mu = .05$
1	.0001	.0018	.0044	.0061
2	.0019	.0065	.0143	.0193
3	.0062	.0122	.0252	.0337
4	.0133	.0194	.0373	.0493
5	.0230	.0291	.0509	.0653
6	.0346	.0412	.0657	.0812
7	.0480	.0551	.0808	.0961
8	.0634	.0703	.0957	.1094
9	.0812	.0868	.1091	.1201
10	.1045	.1056	.1210	.1277

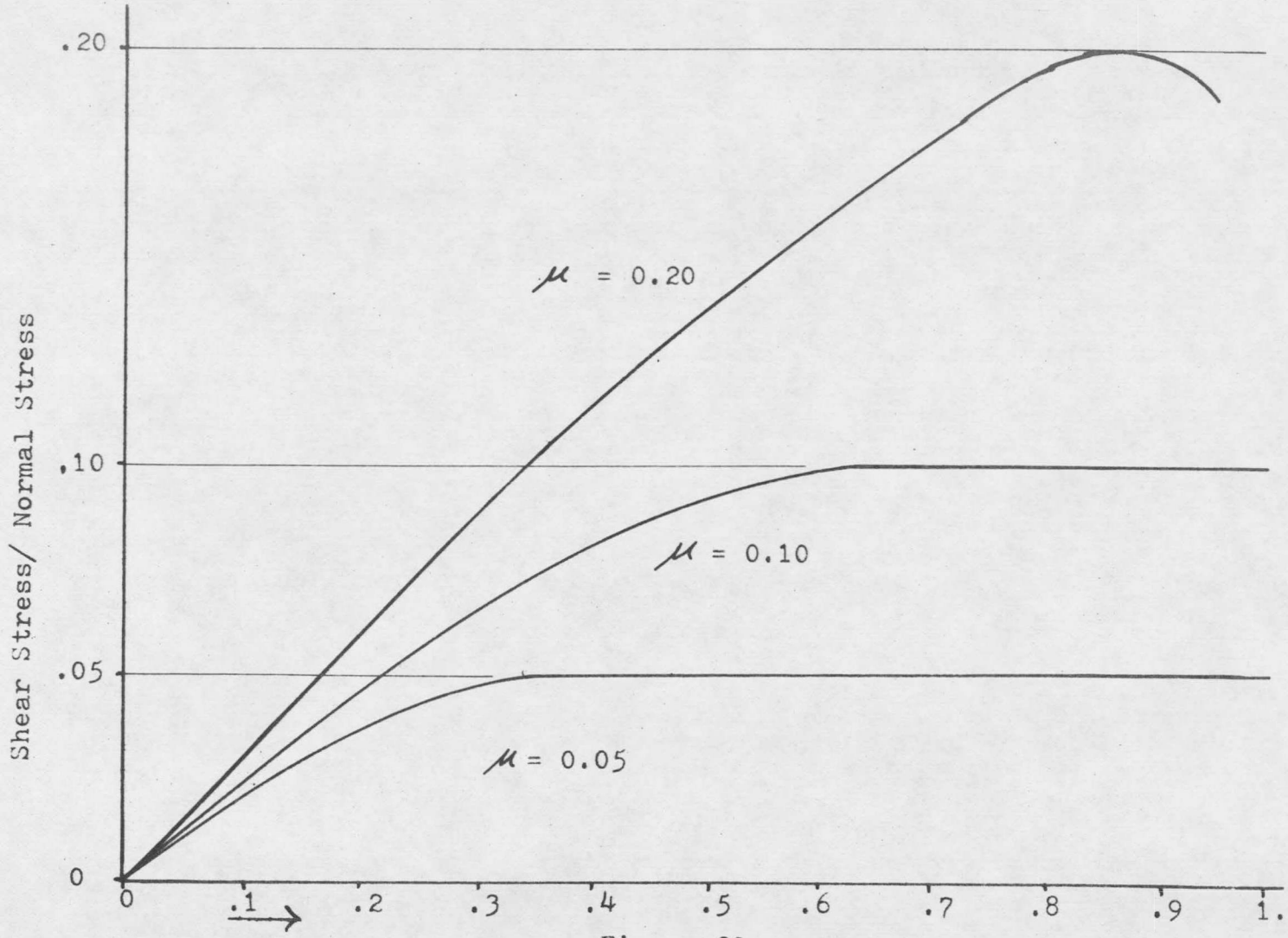

Figure 20
Slip-Stick Regions For Several Coefficients Of Friction

times RC. These also happen to be the radii to the point where the maximum shear stresses occur. See Table 2 or Figure 19.

3.4 Effects Of The Coefficients Of Friction On The Surface Radial Displacements

Listed in Table 4 and plotted in Figure 21 are the radial displacements at the collocation points. The larger the coefficient of friction, the smaller the radial displacements. This is due to the fact that friction between the two bodies tends to keep the half-space surface from being pushed away from the center of the contact region. As was seen in section 3.3 the larger the coefficient of friction, the larger the stick region and the smaller the slip rgion. Therefore the larger the coefficient of friction the less the two bodies are allowed to slip with respect to each other.

3.5 Effects Of The Coefficient Of Friction On The Load And Approach

Listed in Table 5 are the load and approach that have been nondimensionalized with respect to the Hertzian load and approach for the same contact radius. Also listed are maximum normal and shear stresses that have been nondimensionalized with respect to the maximum Hertzian stress

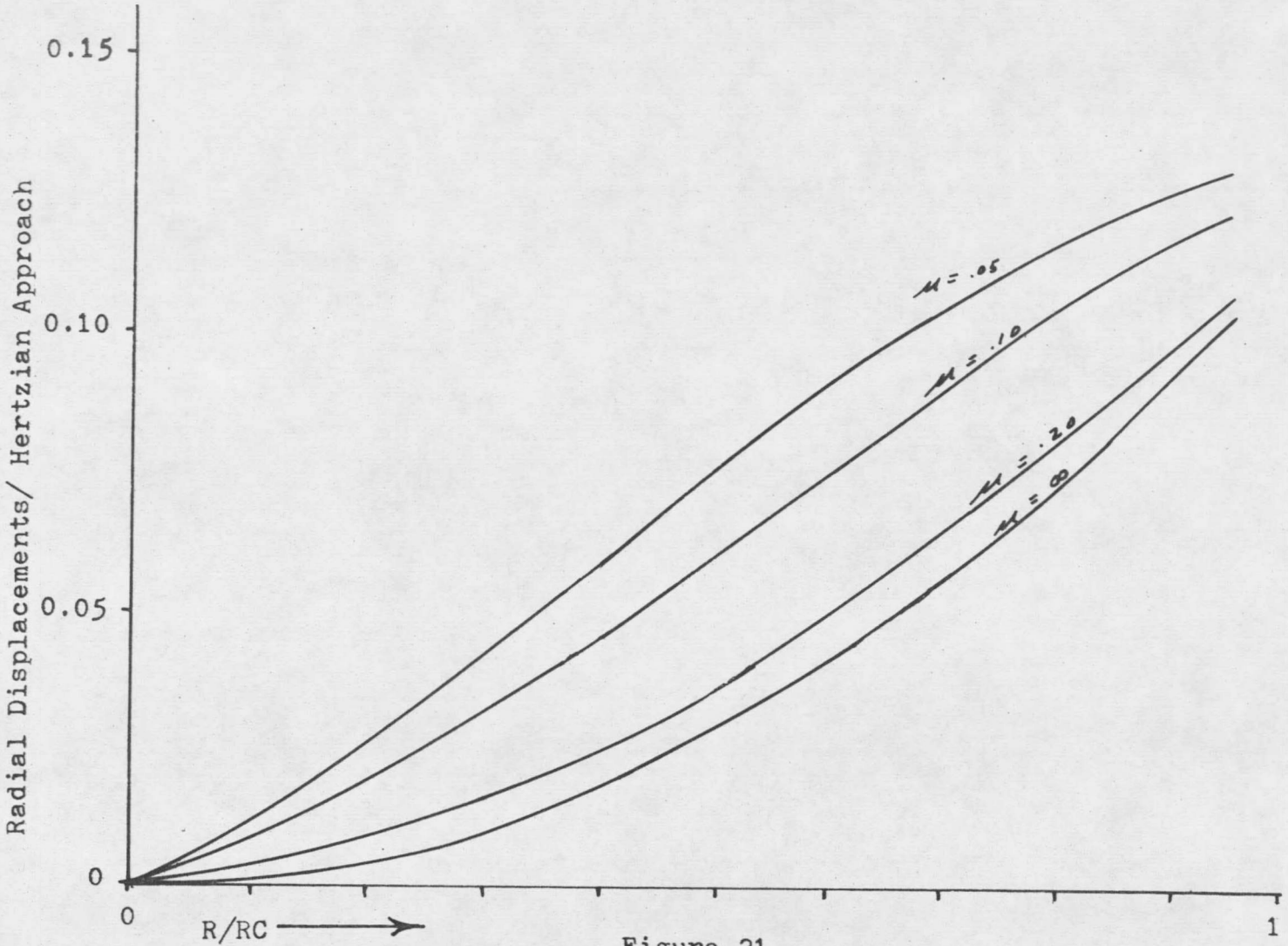

Figure 21

Surface Radial Displacements

Nondimensionalized Quantities*	$\mu = .05$	$\mu = .10$	$\mu = .20$	$\mu = \infty$
Load	1.162	1.217	1.300	1.309
Approach	1.107	1.140	1.191	1.197
Maximum Normal Stress	1.032	1.047	1.070	1.085
Maximum Shear Stress	-.046	-.082	-.140	-.163
Contact Radius	.9512	.9367	.9163	.9142

* Note: The load and approach were nomdimensionalized with resect to the Hertzian values associated with the same contact radius, while the remaining quantities were nondimensionalized with respect to the Hertzian values associated with the same load.

Table 5 Load, Approach, Maximum Stresses and Contact Radius For Several Coefficients Of Friction

associated with the same load. The larger the coefficient of friction, the larger are the load and approach. This is due to the fact that the load is directly proportional to the normal stress and the normal stress increases as the coefficient of friction increases. Since the approach is assumed proportional to the two thirds power of the load (see equation 2.44), the approach also increases as the coefficient of friction increases.

The reason that the maximum normal stress increases as the coefficient of friction increases is due to the fact that the contact region is smaller for a larger coefficient of friction if the same load is applied.

Chapter 4

SUMMARY AND RECOMMENDATIONS

4.1 Summary

The frictional contact problem between a rigid sphere and an elastic half-space has been modeled using a form of the collocation technique in which the surface stresses have been approximated by a series of disk loadings. A computer program has been written using these methods to find the surface shear stresses, the surface normal stresses and the surface displacements for a given set of physical properties and a given coefficient of friction. The effects of various coefficients of friction on the stresses and displacements have been predicted. For the first time it was possible to approximate the surface shear stresses.

4.2 Recommendations

Due to the fact that the problem has been solved by a series of stepwise approximations the error in the magnitudes of any one of the predicted quantities may be a significant amount. The trends in the qualitative results such as an increase in the normal stress with an increase in the coefficient of friction are probably correct.

It was found that for the method used to limit the

shear stress that a coefficient of friction of 0.25 or greater resulted in very nearly the same stresses and displacements as a coefficient of friction of infinity. This is due to the fact that the stresses were approximated by a series of disk loads and the slippage was allowed to take place only inside integer number of regions. It would be desireable if another method could be found that would allow slippage in a non-integer number of regions.

The method that was used to approximate the approach is inexact. As was shown in section 2.6 the error in the approach is less than twelve percent but considering the extremely sensitive nature of the simultaneous equations it is possible a rather small error in the approach could result in large errors in the other quantities. It is recommended that an improved method for finding the approach be devised. It would be best if it were an exact and not an approximate method.

The fact that the stress curves are discontinuous is undesirable. It would be better if smooth curves could be used. Also the way in which the shear stresses are approximated results in rather high values at the outside edge of the contact region where they should be zero. If another method that overcomes these difficulties could be

found it would be desirable.

4.3 Further Applications Of These Methods

Using the general methods developed in this thesis several things could be done to extend the work. Using the surface stresses that were found it would be possible to examine the effects of the coefficient of friction on the interior stresses. This could be done using Boussinesq's equations (see (17), page 364). Also it would be of interest to allow the sphere to roll with respect to the half-space or to replace the half-space by a curved surface that would represent the race of a ball bearing. It is felt that if a method to find the approach exactly could be found that the same methods used in this work could be used to solve contact problems between bodies that were non-conformal and axially symmetric but otherwise entirely arbitrary in shape. Both frictional and frictionless contact problems could be solved.

APPENDIX A

EQUILIBRIUM EQUATIONS FOR AN ELASTIC HALF-SPACE SUBJECTED TO A POINT LOAD APPLIED TO THE FREE SURFACE

Consider an elastic medium occupying a half-space, i.e. bounded on one side by an infinite plane. The surface of the half-space is subjected to a concentrated force F, i.e. one which is applied to an area so small that is can be regarded as a point. Cartesian coordinates are located in the half-space such that the X-Y plane lies on the free surface of the half-space and the Z axis is into the half-space. The point force is applied at the origin. The equations defining the displacements of a point (X,Y,Z) in the half-space are given by Landau and Lifshitz (8) as:

```
UX = (1+S)/(2*PI*E)*((X*Z/R**3 -(1-2*S)*X/R/(R+Z))*FZ
     +(2*(1-S)*R+Z)/R/(R+Z)*FX
     +(2*R*(S*R+Z)+Z**2)*X/R**3/(R+Z)**2*(X*FX+Y*FY))          (A.1)

UY = (1+S)/(2*PI*E)*((Y*Z/R**3 -(1-2*S)*Y/R/(R+Z))*FZ
     + (2*(1-S)*R+Z)/R/(R+Z)*FY
     +(2*R*(S*R+Z)+Z**2)*Y/R**3/(R+Z)**2*(X*FX+Y*FY))          (A.2)

UZ = (1+S)/(2*PI*E)*((2*(1-S)/R + Z**2/R**3)*FZ
     + ((1-2*S)/R/(R+Z) + Z/R**3)*(X*FX+Y*FY))                 (A.3)
```

where UX, UY and UZ are the displacements of a point in the x, y and z directions; FX, FY and FZ are the x, y and z components of the applied force F; E is Young's modulus;

S is Poisson's ratio; R = SQRT(X*X + Y*Y); PI = π; and X, Y and Z are the coordinates of the point.

In particular, the displacements of a point on the surface of the medium are given by putting Z equal to zero in equations A.1, A.2 and A.3.

```
UX = (1+S)/(2*PI*E)/R*(-(1-2*S)*X/R*FZ + 2*(1-S)*FX
     +2*S*X/R**2*(X*FX + Y*FY))                          (A.4)

UY = (1+S)/(2*PI*E)/R*(-(1-2*S)*Y/R*FZ + 2*(1-S)*FZ
     + 2*S*Y/R**2*(X*FX + Y*FY))                         (A.5)

UZ = (1+S)/(2*PI*E)/R*(2*(1-S)*FZ
     +  (1-2*S)/R*(X*FX + Y*FY))                         (A.6)
```

APPENDIX B

NUMERICAL INTEGRATIONS USED TO OBTAIN U1, U2, U3 and U4

Since it was impossible to evaluate the integrals in equations 2.29, 2.30 and 2.31 analytically for all values of R/RD it was necessary to evaluate them by means of numerical integration. Figure B-1 shows the system that was used. The nomenclature that was used is as follows:

RD = Radius of the disk load

R = Radius from the center of the disk load to the collocation point

R1 = Radius from the collocation point to the integration point

R2 = Radius from the center of the disk load to the integration point

$\theta 1$ = Angle between R and R1

$\theta 2$ = Angle between R and R2

X1 = Distance in the x direction from the center of the disk load to the integration point

X2 = Distance in the x direction from the integration point to the collocation point

Y1 = Distance in the y direction from the center of the disk load to the integration point

Y2 = Distance in the y direction from the integration point to the collocation point

dR = Incremental step size in R1 used for integration

$d\theta$ = Incremental step size in $\theta 1$ used for integration

$d\Omega$ = R1*dR*$d\theta$

Ω = the contact region inside R = RC

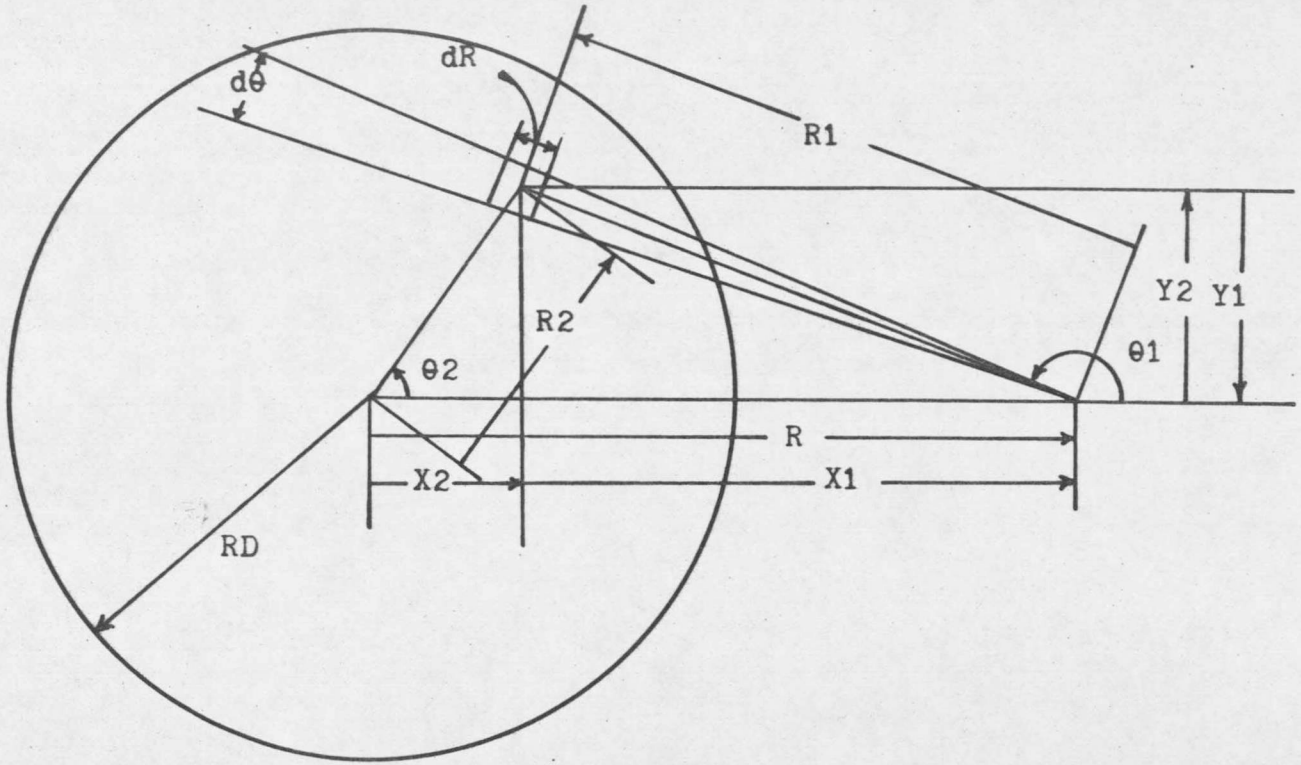

Figure B-1
System Used For Numerical Integrations

U11 = $\int$UXZ*dΩ

U12 = $\int$UXX1*dΩ

U13 = $\int$UXX2*dΩ

U14 = $\int$UXY*dΩ

U21 = $\int$UYZ*dΩ

U22 = $\int$UYY1*dΩ

U23 = $\int$UYY2*dΩ

U24 = $\int$UYX*dΩ

U31 = $\int$UZZ*dΩ

U32 = $\int$UZX*dΩ

U33 = $\int$UZY*dΩ

By using Equations 2.17 through 2.27 and 2.32 through 2.34 these can be rewritten as follows:

U11 = $\int$SZ*X1/R1**2*dΩ = $\int\int$(X1/R1)*dR*dθ = $\int\int$cosθ*dr*dθ

U12 = $\int$SX/R1*dΩ = $\int\int$(X2/RC)*dR*dθ

U13 = $\int$(SX*X1**2/R1**3)*dΩ = $\int\int$(X2/RC)*(cosθ)**2*dR*dθ

U14 = $\int$(SY*X1*Y1/R1**3)*dΩ = $\int\int$(Y2/RC)*cosθ*sinθ*dR*dθ

U21 = $\int$(SZ*Y1/R1**2)*dΩ = $\int\int$sinθ*dR*dθ

U22 = $\int$(SY/R1)*dΩ = $\int\int$(Y2/RC)*dR*dθ

U23 = $\int$(SY*Y1**2/R1**3)*dΩ = $\int\int$(Y2/RC)*(sinθ)**2*dR*dθ

U24 = $\int$(SX*X1*Y1/R1**3)*dΩ = $\int\int$(X2/RC)*sinθ*cosθ*dR*dθ

U31 = $\int$(SZ/R1)*dΩ = $\int\int$dR*dθ

U32 = $\int$(SX*X1/R1**2)*dΩ = $\int\int$(X2/RC)*cosθ*dR*dθ

$$U33 = \int_{\Omega}(SY*Y1/R1**2)*d\Omega = \iint(Y2/RC)*\sin\theta*dR*d\theta$$

Each of the integrals was done numerically for values of R/RD ranging from 0.0 to 4.0. RD was fixed for all integrations since the results will be directly proportional to RD. The value for dR was RD/100 and for dθ was PI/50. θ1 was varied from 0 to 2*PI and R1 was varied from 0 to 5*RC so that all points in the disk loading would be included. If the integration point was outside of the load circle no contribution to the results were added. For each integration point that fell inside the load circle cosθ, sinθ, X2, Y2, dR and dθ were calculated and the incremental contribution added to each displacement.

All of the y components of displacements (U21, U22, U23 and U24) were esentially zero. In addition U13 + U14 was equal to zero and U32 + U33 was equal to zero outside the contact region. The numerical results are given in Table B1 and Figures 7, 8, 9 and 10. In Table B2 are listed the percent errors between the values obtained by numerical integration and the approximations to U1, U2, U3 and U4.

Table B1

R/RD	UZZ/RD	$\frac{UZX+UZY}{RD}$	UXZ/RD	UXX1/RD
.0	6.2832	3.1416	.0000	.0000
.1	6.2694	3.1121	.3135	.3137
.2	6.2166	3.0127	.6300	.6167
.3	6.1424	2.8620	.9423	.9103
.4	6.0205	2.6359	1.2586	1.1757
.5	5.8735	2.3598	1.5708	1.4152
.6	5.6750	2.0131	1.8850	1.6080
.7	5.4186	1.5987	2.1988	1.7402
.8	5.1045	1.1294	2.5129	1.7942
.9	4.6847	.5949	2.8283	1.7171
1.0	3.9999	.0059	3.1410	1.3341
1.1	3.335	.000	2.859	
1.2	2.951	.000	2.622	.695
1.3	2.662	.000	2.421	
1.4	2.434	.000	2.251	.470
1.5	2.242	.000	2.099	
1.6	2.086	.000	1.971	.346
1.7	1.947	.000	1.853	
1.8	1.810	.000	1.735	.265
1.9	1.728	.000	1.662	
2.0	1.614	.000	1.561	.210
2.1	1.553	.000	1.506	
2.2	1.456	.000	1.418	.171
2.3	1.402	.000	1.368	
2.4	1.352	.000	1.321	.143
2.5	1.281	.000	1.254	
2.6	1.225	.000	1.202	.122
2.7	1.190	.000	1.169	
2.8	1.152	.000	1.133	.104
2.9	1.105	.000	1.087	
3.0	1.042	.000	1.028	.090
3.1	1.022	.000	1.008	
3.2	1.002	.000	.989	.078
3.3	.978	.000	.966	
3.4	.947	.000	.937	.069
3.5	.914	.000	.904	
3.6	.849	.000	.842	.062
3.7	.838	.000	.831	
3.8	.827	.000	.820	.056
3.9	.813	.000	.806	
4.0	.799	.000	.793	.050

Table B2

R/RD	Percent Error			
	UZZ/RD	$\frac{UZX+UZY}{RD}$	UXZ/RD	UXX1/RD
.0	-.000	-.000	.000	.000
.1	-.031	-.062	.210	4.348
.2	.053	.107	-.267	4.553
.3	-.050	-.110	.019	3.513
.4	.054	.115	-.156	2.877
.5	-.062	-.153	-.000	1.443
.6	-.047	-.123	-.002	.047
.7	.074	.220	.014	-1.431
.8	.017	.139	.015	-3.151
.9	.044	.336	-.031	-4.057
1.0	.002	.000	.019	-.057
1.1	-.085	.000	-.105	
1.2	-.242	.000	-.153	-.770
1.3	-.270	.000	-.181	
1.4	-.358	.000	-.311	-.409
1.5	-.250	.000	-.219	
1.6	-.422	.000	-.381	-.763
1.7	-.324	.000	-.270	
1.8	.663	.000	.595	-.312
1.9	-.595	.000	-.513	
2.0	.693	.000	.628	.087
2.1	-.676	.000	-.664	
2.2	.830	.000	.705	.299
2.3	-.089	.000	-.153	
2.4	-.929	.000	-.909	-.160
2.5	.189	.000	.210	
2.6	.571	.000	.525	-.996
2.7	-.453	.000	-.466	
2.8	-.971	.000	-.971	-.417
2.9	-.436	.000	-.340	
3.0	1.957	.000	1.867	-.204
3.1	.504	.000	.537	
3.2	-.778	.000	-.733	.843
3.3	-1.499	.000	-1.450	
3.4	-1.338	.000	-1.388	.680
3.5	-.760	.000	-.708	
3.6	3.809	.000	3.642	-.303
3.7	2.274	.000	2.176	
3.8	.859	.000	.821	-1.135
3.9	-.080	.000	-.058	
4.0	-.913	.000	-.959	-.243

APPENDIX C

Listed in this appendix is a copy of the program that was used to determine the surface displacements of a half-space subjected to the stress distribution discussed in section 2.5. The methods that were used to do the numerical integrations is similar to those described in Appendix B.

```
      DIMENSION R(21),UX(21),UY(21),UZ(21)
      NR=20;NT1=2
      RC=0.02545
      PI=3.14159265358973
      E=30.E06
      S=0.3
      A1=(1.+S)/(2.*PI*E)
      A2=(1.-2.*S)
      A3=2.*(1.-S)
      A4=2.*S
      DO 20 I=1,10
      R(I)=RC*((I-.5)/10.)
      UX(I)=0.0
      UZ(I)=0.0
      DR=RC/NR
      DO 10 II=1,NR
      R1=RC/NR*SQRT((2.*II*II-2.*II+1.)/2.)
      DT=PI/(NT1*(II*2.-1))
      DO 10 III=1,(2*II-1)*NT1
      T1=DT*(III-.5)
      C1=COS(T1)
      S1=SIN(T1)
      R2=SQRT((R(I)+R1)**2.-2.*R(I)*R1*(1.-C1))
      IF (R2.GT.RC) GO TO 10
      T2=ATAN(R1*S1,(R1*C1-R(I)))
      UX(I)=UX(I)+(A1*(-A2*FZ(R2)*C1+A3*FX(R2,T2)
     & +A4*FX(R2,T2)*C1*C1+A4*FY(R2,T2)*C1*S1))*DR*DT
      UZ(I)=UZ(I)+(A1*(A3*FZ(R2)+A2*FX(R2,T2)*C1
     & +A2*FY(R2,T2)*S1))*DR*DT
   10 CONTINUE
      UX(I)=UX(I)*2.
      UZ(I)=UZ(I)*2.
   20 WRITE (103,11) R(I),UZ(I),UX(I)
   11 FORMAT (3(1X,1PE11.4))
      END
```

```
      REAL FUNCTION FZ(R2)
      P=5.76E5
      RC=0.02545
      FZ=P*COS(3.14159265/2.*(R2/RC))
      RETURN
      END
      REAL FUNCTION FX(R2,T2)
      Q=1.6E05
      RC=0.02545
      FX=COS(T2)*Q*SIN(3.14159265*(R2/RC))
      RETURN
      END
      REAL FUNCTION FY(R2,T2)
      Q=1.6E05
      RC=0.02545
      FY=SIN(T2)*Q*SIN(3.14159265*(R2/RC))
      RETURN
      END
```

APPENDIX D

Listed in this appendix is a copy of the main program that was used to solve the frictional contact problem of a rigid sphere in contact with an elastic half-space. The parameters that are used are defined in the program. The subroutines E and K are elliptic integrals of the first and second kind respectively. Function F is the profile function between a sphere and a half-space. Functions U1, U2, U3 and U4 are the displacements due to the disk loads as described in section 2.3. Subroutine GAUSED is used to solve the simultaneous equations by Gauss-Seidel iteration.

```
!JOB 769,ALZHEIMER,1
!LIMIT (TIME,10),(CORE,6),(UO,120)
!FORTRAN GO,NS,ADP
C     MAINLINE TO SOLVE FOR NORMAL AND SHEAR STRESSES
C      BETWEEN RIGID SPHERE AND ELASTIC HALFSPACE
C
      DIMENSION RC(10),RA(10),STRESS(20),DISP(20),A(20,21)
      DIMENSION HERTZ(20),X(20),RCA(10)
      COMMON E1,S,PI
      COMMON FAC
      REAL LOAD,MU,II,NN
C     NOW DEFINE ALL PARAMETERS
C     ITMAX=MAXIMUM # OF ITERATIONS ALLOWED IN SOLVING EQS
C     E1=YOUNG'S MODULUS OF HALF-SPACE
C     S=POISON'S RATIO OF HALF-SPACE
C     MU=FRICTION COEFFICIENT BETWEEN SPHERE AND HALF-SPACE
C     R1=RADIUS OF SPHERE
C     R2=RADIUS OF CONTACT AREA
C     R2START,R2STEP & R2STOP ARE USED TO INCREASE APPROACH
C     N=NUMBER OF COLLOCATION POINTS
C     FAC IS USED TO DETERMINE LOAD VS APPROACH
C     RC=RADIUS TO COLLOCATION POINTS
C     RA=RADIUS OF DISK LOADS
C     STRESS=CALCULATED STRESS, BOTH SHEAR AND NORMAL
C     DISP=DISPLACEMENTS OF HALF-SPACE SURFACE
C     X=MAGNITUDE OF INDIVIDUAL DISK LOADS
C     HERTZ=STRESSES PREDICTED BY HERTZ
C     A = COEFFICIENT MATRIX
C     P & PO ARE LOAD AND MAX STRESS PREDICTED BY HERTZ
C     EPS=TOLERANCE USED IN SOLVING EQUATIONS
C     GAUSED IS THE SUBROUTINE USED TO SOLVE EQUATIONS
C     GAUSED USES GAUSS-SEIDEL ITERATION
C     S1,S2 AND S3 ARE USED TO CHECK AND LIMIT SHEAR STRESSES
C     LOAD IS THE TOTAL LOAD APPLIED TO THE SPHERE
C     APP IS THE APPROACH BETWEEN THE SPHERE AND HALF-SPACE
      ITMAX=200
      E1=30.E6
      S=0.3
      MU=0.05
      R1=1.0
      PI=3.14159265
      R2START=0.0005
      R2STEP=0.0005
      R2STOP=0.02
```

```
      N=10
      N2=2*N
      NN=N
      FAC=1.00
      OUTPUT N,E1,S,MU,ITMAX,R1,R2START,R2STOP,R2STEP
C     ALL ARRAYS ARE ZEROED
      DO 12 I=1,N
      RC(I)=0.0;RA(I)=0.0;RCA(I)=0.0
   12 CONTINUE
      DO 10 I=1,N2
      STRESS(I)=0.0
      DISP(I)=0.0
      X(I)=0.0
      HERTZ(I)=0.0
      DO 10 J=1,N2+1
   10 A(I,J)=0.0
      R2=R2START
    1 CONTINUE
C
C     RADII OF AREAS AND RADII OF COLLOCATION POINTS
C     ARE NOW ESTABLISHED
C
      DO 20 I=1,N
      II=I
      RC(I)=R2*((II-.5)/NN)
   20 RA(I)=R2*II/NN
C     NOW CALCULATE NORMAL STRESSES AT COLLOCATION
C     POINTS FOR THE CASE WHERE THERE IN NO FRICTION.
C     THIS WILL BE USED AS THE FIRST GUESS OF THE
C     TRUE STRESS DISTRIBUTION
C
      P=(R2/.880)**3./(R1*(1./E1))
      PO=0.616*(P*(E1/R1)**2.)**(1./3.)
      EPS=0.0001*PO
      DO 30 I=1,N
      HERTZ(I)=PO*2./3.*((1.-((I-1)/N)**2.)**1.5
     &-(1.-(I/N)**2.)/((2.*I-1.)/N*N)*N*N
   30 HERTZ(I+N)=0.0
C
C     NOW DISPLACEMENTS AT COLLOCATION PTS. ARE
C     CALCULATED FOR DISKS OF UNIT MAGNITUDES
      DO 3 IFAC=1,5
      DO 40 I=1,N
```

```
      DO 40 J=1,N
      R=RC(I)
      A1=RA(J)
      A(I,J)=U1(R,A1)
      A(I,J+N)=U2(R,A1)
      A(I+N,J)=U3(R,A1)
   40 A(I+N,J+N)=U4(R,A1)
C
C
      DO 60 I=1,N
      A(I,N2+1)=F(RC(I),R1,R2)
   60 A(I+N,N2+1)=DISP(I+N)
      CALL GAUSED (A,X,N2,ITMAX,EPS)
      DO 70 I=1,N2
   70 STRESS(I)=0.0
      DO 80 I=1,N
      DO 80 J=I,N
   80 STRESS(I)=STRESS(I)+X(J)
      STRESS(N2)=X(N2)
      DO 90 I=N-1,1,-1
   90 STRESS(I+N)=STRESS(I+N+1)*RA(I)/RA(I+1)+X(I+N)
C     NOW SHEAR STRESSES ARE CHECKED AND LIMITED
      DO 102 I=1,N
      II=I
      S1=STRESS(I)
      S2=STRESS(I+N)*(II-.5)/II
      S3=ABS(S2)
      IF(S3.GT.S1*MU) STRESS(I+N)=S1*MU*S2/S3*II/(II-.5)
  102 CONTINUE
      LOAD =0.0
      DO 33 I=1,N
   33 LOAD = LOAD + PI*X(I)*RA(I)*RA(I)
      HLOAD=LOAD*R1*3./4.*(1.-S*S)/(R2**3.*E1)
C     A NEW GUESS IS MADE FOR THE APPROACH
      FAC=6.0*(HLOAD)**(2./3.)-5.0*FAC
    3 CONTINUE
    4 CONTINUE
C     DISPLACEMENTS AT THE NEW COLLOCATION POINTS
C     ARE CALCULATED USING STRESSES
      R2A=R2+R2STEP
      X(N2)=STRESS(N2)
      DO 105 I=N-1,1,-1
      II=I
      X(I+N)=STRESS(I+N)-STRESS(I+N+1)*II/(II+1)
  105 CONTINUE
```

```
      DO 110 I=1,N
      II=I
  110 RCA(I)=R2A*((II-.5)/NN)
      DO 100 I=1,N2
  100 DISP(I)=0.0
      DO 120 I=1,N
      DO 120 J=1,N
      R=RCA(I);A1=RA(J)
      DISP(I)=DISP(I)+X(J)*U1(R,A1)+X(J+N)*U2(R,A1)
  120 DISP(I+N)=DISP(I+N)+X(J)*U3(R,A1)+X(J+N)*U4(R,A1)
      WRITE (108,200) R2
      OUTPUT ' ','STRESS AFTER SLIP'
      WRITE (108,201) (STRESS(I),I=1,N2)
      OUTPUT ' ','HERTZIAN STRESS'
      WRITE (108,201) (HERTZ(I),I=1,N)
      OUTPUT ' ', 'NORMAL STRESS/ HERTZIAN STRESS'
      WRITE (108,202) (STRESS(I)/HERTZ(I),I=1,N)
      OUTPUT ' ','STRESS / MAX HERTZIAN STRESS'
      WRITE(108,202) (STRESS(I)/P0,I=1,N2)
      OUTPUT ' ','SHEAR / NORMAL'
      WRITE (108,202) (STRESS(I+N)/STRESS(I),I=1,N)
      OUTPUT ' ','DISPLACEMENTS'
      WRITE (108,203) (DISP(I),I=1,N2)
      OUTPUT ' ','DISP*R1/R2**2'
      WRITE(108,202) (DISP(I)*R1/R2**2.,I=1,N2)
      APP=0.0
      DO 101 I=1,N
  101 APP=APP+X(I)*U1(0.0,RA(I))+X(I+N)*U2(0.0,RA(I))
      APP1=APP*R1/R2**2.
      OUTPUT ' '
      WRITE(108,204) APP1
      OUTPUT ' '
      WRITE(108,205) HLOAD
      IF (R2.GT.R2STOP) GO TO 999
      R2=R2+R2STEP
      GO TO 1
    2 CONTINUE
  999 CONTINUE
```

```
200 FORMAT ('1','RADIUS OF CONTACT IS NOW =',2X,F7.4)
201 FORMAT (10(1X,F10.2))
202 FORMAT (10(1X,F10.6))
203 FORMAT (10(1PE11.4))
204 FORMAT('APPROACH / HERTZIAN APPROACH =     ',F10.6)
205 FORMAT('LOAD / HERTZIAN LOAD =     ',F10.6)
    END




    REAL FUNCTION E(M1)
    REAL M1
    A1=0.44325141463
    A2=0.06260601220
    A3=0.04757383546
    A4=0.01736506451
    B1=0.24998368310
    B2=0.09200180037
    B3=0.04069697526
    B4=0.00526449639
    E=(1.+A1*M1+A2*M1*M1+A3*M1*M1*M1+A4*M1*M1*M1*M1)
   & +LOG(1./M1)*(B1*M1+B2*M1*M1+B3*M1*M1*M1+B4*M1*M1*M1*M1)
    RETURN
    END
    REAL FUNCTION K(M1)
    REAL M1
    C0=1.38629436112
    C1=0.09666344259
    C2=0.03590092383
    C3=0.03742563713
    C4=0.01451196212
    D0=0.5
    D1=0.12498593597
    D2=0.06880248576
    D3=0.03328355346
    D4=0.00441787012
    K=(C0+C1*M1+C2*M1*M1+C3*M1*M1*M1+C4*M1*M1*M1*M1)
   & +(D0+D1*M1+D2*M1*M1+D3*M1*M1*M1+D4*M1*M1*M1*M1)*LOG(1./M1)
    RETURN
    END
```

```
      REAL FUNCTION F(R,R1,R2)
      COMMON E1,S,PI,FAC
      F=R2*R2/R1*FAC+SQRT(R1*R1-R*R)-R1
      RETURN
      END

      REAL FUNCTION U1(R,A)
      COMMON E1,S,PI
      REAL K,M1
      IF (R.GT.A) GO TO 10
      M1=1.-(R/A)**2.
      U1=A*E(M1)*4.*(1.-S*S)/(PI*E1)
      GO TO 20
   10 M1=1.-(A/R)**2.
      U1=(R*(E(M1)-M1*K(M1))*4.)*(1.-S*S)/(PI*E1)
   20 CONTINUE
      RETURN
      END
      REAL FUNCTION U2(R,A)
      COMMON E1,S,PI
      IF (R.GT.A) GO TO 10
      U2=PI*(A*A-R*R)/A*(1.+S)*(1.-2.*S)/(2.*PI*E1)
      GO TO 20
   10 U2=0.0
   20 CONTINUE
      RETURN
      END

      REAL FUNCTION U3(R,A)
      COMMON E1,S,PI
      IF (R.GT.A) GO TO 10
      U3=PI*R*(1.+S)*(1.-2.*S)/(2.*PI*E1)
      GO TO 20
   10 U3=PI*A*A/R*(1.+S)*(1.-2.*S)/(2.*PI*E1)
   20 CONTINUE
      RETURN
      END
```

```
      REAL FUNCTION U4(R,A)
      COMMON E1,S,PI
      REAL K,M1
      IF (R.GT.A) GO TO 10
      M1=1.-(R/A)**2.
      U4=4./3.*K*E(M1)*E(M1)*(1.0-S*S)/(PI*E1)
      GO TO 20
   10 M1=1.-(A/R)**2.
      U4=4./PI*R*R/A*(E(M1)-M1*K(M1))**2.*(1.-S*S)/(PI*E1)
   20 CONTINUE
      RETURN
      END


      SUBROUTINE GAUSED(A,X,N,ITMAX,EPS)
      INTEGER FLAG
      DIMENSION A(20,21),X(20)
      NP1=N+1
      DO 3 I=1,N
      ASTAR=A(I,1)
      DO 3 J=1,NP1
    3 A(I,J)=A(I,J)/ASTAR
      DO 9 ITER =1,ITMAX
      FLAG=1
      DO 7 I=1,N
      XSTAR=X(I)
      X(I)=A(I,NP1)
      DO 5 J=1,N
      IF (I .EQ. J) GO TO 5
      X(I)=X(I)-A(I,J)*X(J)
    5 CONTINUE
      IF(ABS(XSTAR-X(I)) .LE. EPS) GO TO 7
      FLAG =0
    7 CONTINUE
      IF (FLAG.NE.1) GO TO 9
      OUTPUT ITER
      GO TO 1
    9 CONTINUE
      OUTPUT 'DID NOT CONVERGE'
    1 CONTINUE
      RETURN
      END
!LOAD (GO)
!RUN
!EOD
```

BIBLIOGRAPHY

1. Abramowitz, M. and Stregun, I.A., Handbook of Mathmatical Functions, U.S. Department of Commerce, National Bureau of Standards, Applied Mathmatics Series 55 (1964)

2. Blackketter, D.O., Contact Stresses Between Two-dimensional Elastic Bodies, PhD dissertation, University of Arizona (1966)

3. Carnahan, B, Luther, H.A. and Wilkes, J.O., Applied Numerical Methods, John Wilet and Sons, Inc., (1969)

4. Cattaneo, C., Teoria del contacto elastico in seconda approxximazione, Univ. Rome, Rend. Mat. Appl., 6, 540-512 (1947)

5. Conry, T.F. and Seireg, A., A mathematical programming method for design of elastic bodies in contact, Journ. of Appl. Mech., Trans. of ASME E 38, 387-392(Jan. 1971)

6. Hertz, H., Miscellaneous papers (Trans. by D.E. Jones and G.A. Schott) Macmillan and Co., London (1896) Translated from (i) On the contact of elastic solids, Journal furr die reine und angewandte mathematik, 92, 156-171 (1881) (ii) On the contact of rigid elastic solids and on hardness, Verhandlungen des Vereins zur Befordrung des Gewerbefleisses, (Nov. 1882)

7. Kalker, J.J. and Van Randen, Y., A minimum principle for frictionless elastic contact with application to non-Hertzian half-space contact problems, Journ. of Engineering Math., April 1972

8. Landau, L.D. and Lifshitz, E.M., Theory of Elasticity, Addison-Wesley, (1959)

9. Love, A.E.H., Mathmatical Theory Of Elasticity, Dover, N.Y. (1927)

10. Lubkin, J.L., Contact Problems, Handbook of Engineering Mechanics, ed. by Fugge, McGraw-Hill (1962)

11. Malvern, L.E., Introduction to the Mechanics of a Continuous Medium, Prentice-Hall (1969)

12. Magenau, H and Murphy, G.M., The Mathmatics of Physics and Chemistry, 2nd ed., D. Van Nostrand Co., Inc. (1961)

13. Mow, V.C., Chow, P.L. and Ling, F.F., Microslips between contacting paraboloids, JAM, Trans of the ASME, Series E, 2, 89, 321-378 (June 1967)

14. Seely, F.B. and Smith, J.O., Advanced Mechanics of Materials, 2nd ed., John Wiley and Sons, Inc. (1952)

15. Singh, K.P., Contact Stresses in Bodies With Arbirary Profiles, PhD dissertation, University of Pennsylvania (1972)

16. Spotts, M.F., Design of Machine Elements, 4th ed., Prentice-Hall (1971)

17. Timoshenko, S.P. and Goodier, J.N., Theory of Elasticity, 2nd ed., McGraw-Hill (1951)

18. Tuve, G.L. and Boltz, R.E., Handbook of Tables for Applied Engineering Science, The Chemical Rubber Co., (1970)

19. Wylie, C.R., Advanced Engineering Mathmatics, 3rd ed., McGraw-Hill (1966)

Alzheimer, James M
Normal and shear stresses between a rigid sphere and an elastic half-space